

Disclaimer: The manuscript and its contents are confidential, intended for journal review purposes only, and not to be further disclosed.

URL: <https://circ-submit.aha-journals.org/>

Manuscript Number: CIRCULATIONAHA/2022/062193D

Title: Transcriptional dysregulation underlies both a monogenic arrhythmia syndrome and common modifier of cardiac repolarization

Disclaimer: The manuscript and its contents are confidential, intended for journal review purposes only, and not to be further disclosed.

Authors:

Kevin Bersell (Brigham and Women's Hospital)
Tao Yang (Vanderbilt University Medical Center)
Jonathan Mosley (Vanderbilt University Medical Center)
Andrew Glazer (Vanderbilt University Medical Center)
Andrew Hale (Vanderbilt University)
Dmytro Kryshtal (Vanderbilt University Medical Center)
Kyungsoo Kim (Vanderbilt University Medical Center)
Jeffrey Steimle (University of Chicago)
Jonathan Brown (Vanderbilt University Medical Center)
Joe-Elie Salem (APHP.Sorbonne)
Courtney Campbell (The Ohio State University Wexner Medical Center)
Charles Hong (Univ. of Maryland School of Medicine)
Quinn Wells (Vanderbilt University Medical Center)
Amanda Johnson (Vanderbilt University)
Laura Short (Vanderbilt University Medical Center)
Marcia Blair (Vanderbilt University Medical Center)
Elijah Behr (St George's University of London)
Evmorfia Petropoulou (AlfaLab)
Yalda Jamshidi (St. George's University of London)
Mark Benson (Beth Israel Deaconess Medical Center)
Michelle Keyes (Beth Israel Cardiovascular Institute)
Debby Ngo (Beth Israel Deaconess Med Center)
Ramachandran Vasan (Boston University School of Medicine)
Qiong Yang (Boston Univ School of Public Health)
Robert Gerszten (Beth Israel Deaconess Medical Center)
Christian Shaffer (Vanderbilt University Medical Center)
Shan Parikh (Vanderbilt University Medical Center)
Quanhu Sheng (Vanderbilt University Medical Center)
Prince Kannankeril (Vanderbilt University Medical School)
Ivan Moskowitz (University of Chicago)
John York (Vanderbilt University)
Thomas Wang (University of Texas Southwestern Medical Center)
Bjorn Knollmann (Vanderbilt University Medical Center)
Dan Roden (Vanderbilt Univ. School of Medicine)

Transcriptional dysregulation underlies both a monogenic arrhythmia syndrome and
common modifier of cardiac repolarization

Kevin R. Bersell, MD, PhD¹, Tao Yang, PhD², Jonathan D. Mosley, MD, PhD², Andrew M. Glazer, PhD¹, Andrew T. Hale, PhD³, Dmytro O. Kryshtal, PhD¹, Kyungsoo Kim, PhD¹, Jeffrey D. Steimle, BS,⁸ Jonathan D. Brown, MD², Joe-Elie Salem, MD^{1,2,9}, Courtney C. Campbell, MD, PhD¹, Charles C. Hong, MD, PhD⁷, Quinn S. Wells, MD^{1,2}, Amanda N. Johnson, PhD⁴, Laura Short, MS², Marcia A. Blair, MS², Elijah R. Behr, MD¹¹, Evmorfia Petropoulou, PhD¹⁰, Yalda Jamshidi, MD¹⁰, Mark D. Benson, MD^{11,14}, Michelle J. Keyes, PhD¹¹, Debby Ngo, PhD¹², Ramachandran S. Vasam, PhD¹⁵, Qiong Yang, PhD¹⁵, Robert E. Gerszten, MD^{11,12}, Christian Shaffer, MS², Shan Parikh, MD, PhD¹, Quanhu Sheng, MS⁵, Prince J. Kannankeril, MD⁶, Ivan P. Moskowitz, MD, PhD⁸, John D. York, PhD³, Thomas J. Wang, MD², Bjorn C. Knollmann, MD, PhD^{1,2}, Dan M. Roden, MD^{1,2,5}

Affiliations: Departments of Pharmacology,¹ Medicine,² Biochemistry,³ Molecular Physiology and Biophysics,⁴ Biomedical Informatics,⁵ and Pediatrics.⁶ Vanderbilt University, Nashville, TN, USA; Department of Medicine, University of Maryland School of Medicine, Baltimore, MD, USA;⁷ Departments of Pediatrics, Pathology, and Human Genetics, University of Chicago, Chicago, IL, USA;⁸ AP-HP, Pitié-Salpêtrière Hospital, Department of Pharmacology; INSERM, CIC-1421 and UMR ICAN 1166, Paris, France; Sorbonne Universités, UPMC Univ Paris 06, Faculty of Medicine, France;⁹

Cardiology Clinical Academic Group, Molecular and Clinical Sciences Institute, St George's, University of London and St. George's University Hospitals NHS Foundation Trust, London, UK;¹⁰ Cardiovascular Research Center, Beth Israel Deaconess Medical Center, Boston, MA;¹¹ Division of Pulmonary¹² and Cardiovascular Medicine, Beth Israel Deaconess Hospital, Boston, MA, USA;¹³ Division of Cardiovascular Medicine, Brigham and Women's Hospital, Boston, MA;¹⁴ Boston University School of Medicine, Boston, MA, USA;¹⁵

Running title: Impaired TBX5 signaling increases arrhythmia risk

Corresponding author:

Dan M. Roden, MD

Vanderbilt University Medical Center

2215B Garland Ave, 1285 MRBIV Light Hall

Nashville, TN 37232-0575

dan.roden@vumc.org

Tel: (615) 322-0067

Fax: (615) 343-4522

Total word count: 5,213

Abstract

Background: The Brugada syndrome (BrS) is an inherited arrhythmia syndrome caused by loss-of-function variants in the cardiac sodium channel gene *SCN5A* in ~20% of subjects. We identified a family with four individuals diagnosed with BrS harboring the rare G145R missense variant in the cardiac transcription factor *TBX5* and no *SCN5A* variant.

Methods: We generated induced pluripotent stem cells (iPSCs) from two members of a family carrying *TBX5*-G145R and diagnosed with Brugada syndrome. After differentiation to cardiomyocytes (iPSC-CMs), electrophysiologic characteristics were assessed by voltage- and current-clamp experiments (n=9-21 cells per group) and transcriptional differences by RNA sequencing (n=3 samples per group), and compared to iPSC-CMs in which G145R was corrected by CRISPR/Cas9 approaches. The role of platelet derived growth factor (PDGF)/PI3K pathway was elucidated by small molecule perturbation. QTc association with serum PDGF was tested in the Framingham Heart Study Cohort (n=1,893 individuals).

Results: *TBX5*-G145R reduced transcriptional activity and caused multiple electrophysiologic abnormalities, including decreased peak and enhanced “late” cardiac sodium current (I_{Na}), which were entirely corrected by editing G145R to wild-type. . Transcriptional profiling and functional assays in genome unedited and edited iPSC-CMs showed direct *SCN5A* down-regulation caused decreased peak I_{Na} , and that reduced PDGF receptor (*PDGFRA*) expression and blunted signal transduction to phosphoinositide 3-kinase (PI3K) was implicated in enhanced late I_{Na} . Both *Tbx5* regulation of the PDGF axis and disruption of PDGF signaling causing arrhythmia risk

were conserved in murine model systems. PDGF receptor blockade markedly prolonged normal iPSC-CM action potentials and plasma levels of PDGF in the Framingham Heart Study were inversely correlated with QTc ($P < 0.001$).

Conclusions: These results not only establish decreased *SCN5A* transcription by the *TBX5* variant as a cause of Brugada syndrome, but also reveal a new general transcriptional mechanism of arrhythmogenesis of enhanced late sodium current caused by reduced PDGF receptor-mediated PI3K signaling.

Keywords: Brugada syndrome, stem cells, arrhythmia, genetics

Disclaimer: The manuscript and its contents are confidential, intended for journal review purposes only, and not to be further disclosed.

Clinical Perspective

What is new?

- Using CRISPR/Cas9 editing in patient-derived induced pluripotent stem cells, we establish a missense variant in the transcription factor gene *TBX5* as a cause of Brugada syndrome.
- We also show that these cells demonstrate reduced platelet derived growth factor (PDGF) receptor-mediated signaling resulting in enhanced late sodium current and prolonged action potentials; this effect is phenocopied by PDGF receptor inhibition in wild-type cells.

What are the clinical implications?

- Tyrosine kinase inhibitors with activity against the PDGF receptor may result in QT prolongation and increased arrhythmia risk.
- Data from the Framingham Heart study support the idea that serum PDGF is a modifier of human QTc, and thus may be a biomarker for arrhythmia risk.

Abbreviations

APA	action potential amplitude
APD	action potential duration
APD ₅₀	action potential duration at 50% repolarization
APD ₉₀	action potential duration at 90% repolarization
BrS	Brugada syndrome
cLQTS	congenital long QT syndrome
EB	embryoid bodies
EFP	extracellular field potentials
EP	electrophysiology
FDP	field potential duration
FHS	Framingham Heart Study
gRNA	guide RNA
HEK	human embryonic kidney
HOS	Holt-Oram syndrome
ICD	implantable cardioverter defibrillator
Indel	insertion or deletion
iPSC	induced pluripotent stem cell
iPSC-CM	induced pluripotent stem cell-derived cardiomyocytes
I _{Kr}	delayed rectifying potassium currents
I _{Ks}	slow delayed rectifying potassium currents
I _{Na}	sodium current
I _{Na-L}	late component of sodium current

LOF	loss-of-function
LTV	long term variability
PA	posteroanterior
PI3K	phosphoinositide 3-kinase
PDGF	platelet derived growth factor
RMP	resting membrane potential
RNZ	ranolazine
SR	sarcoplasmic reticulum
STV	short term variability
TA	triggered action potentials
TKI	tyrosine kinase inhibitor
QTc	corrected QT interval

Disclaimer: The manuscript and its contents are confidential, intended for journal review purposes only, and not to be further disclosed.

Introduction

Studies of familial cardiac arrhythmia syndromes have used heterologous expression of ion channels and their ancillary subunits to validate causative genomic variants by demonstrating that they alter protein function in ways consistent with known physiology. More recently, cardiomyocytes from induced pluripotent stem cells (iPSC-CMs) derived from patients with these diseases have been used to confirm conventionally accepted mechanisms. For example, heterologous expression has shown that long QT syndrome-associated variants in cardiac potassium channels decrease K^+ current, and studies in iPSC-CMs demonstrate the expected action potential prolongation. In addition, CRISPR/Cas9 gene editing in iPSC-CMs has been used to further validate variants in known Mendelian disease genes, such as *SCN5A* in the Brugada Syndrome (BrS)¹ and *PLN* in dilated cardiomyopathy.²

BrS is an inherited arrhythmia disease with a characteristic electrocardiogram and an increased risk of sudden cardiac death due to ventricular fibrillation.^{3,4} Genotype-phenotype studies have identified decreased peak sodium current due to abnormal gating or reduced cell surface expression as a common cellular electrophysiologic hallmark of BrS.^{5,6} Loss-of-function variants in the voltage-gated cardiac sodium channel gene *SCN5A* are the most common genetic cause of BrS,⁷ but are identified in only ~20% of cases.^{8,9}

In a family with BrS and no *SCN5A* mutation, we previously reported the identification of a novel missense variant of unknown significance in the gene encoding the cardiac transcription factor TBX5 (c.G433A, p.G145R; **Fig 1a and 1b**).¹⁰ TBX5 is known to modulate *SCN5A* expression,¹¹ and common variants in this gene have been

implicated by genome-wide association studies as modulators of QRS duration, an electrocardiographic correlate of cardiac conduction, slowed in BrS.¹² *TBX5* variants resulting in *TBX5* haploinsufficiency or severe alterations in DNA binding (*e.g.* *TBX5*-G80R) cause the Holt-Oram syndrome (HOS),¹³ a rare disease with abnormal development of the upper limbs and the heart. In mice, *Tbx5* haploinsufficiency phenocopies HOS-related impaired septation and abnormal limb development, and decreases cardiac expression of gap junction proteins, atrial natriuretic peptide, and the cardiac sodium channel.^{14, 15} However, the functional effects of *TBX5* variants associated with less severe alterations in DNA binding have not been established and no causal relationship with BrS has previously been reported. Here we use gene editing in patient-specific iPSC-CMs to prove that *TBX5*-G145R causes familial BrS. Transcriptional profiling and follow-up functional studies identify a *TBX5*-regulated arrhythmogenic network centered on phosphoinositide 3-kinase (PI3K)-mediated signaling.

Methods:

Patient enrollment and study approval: This study was reviewed and approved by the Institutional Review Board at Vanderbilt University Medical Center (Nashville, TN).

Detailed protocols are available in Supplemental Material. iPSC-derived cardiomyocyte RNA-sequencing reads are available in the NCBI Short Read Archive with accession number XX. Murine cardiomyocyte RNA-sequencing raw data was deposited in GEO with an accession number GSEXXXXX.

Statistical analyses:

Electrophysiology and Biochemistry Statistics: Data are mean \pm SEM unless otherwise indicated. Statistical differences among two groups were tested with two-tailed Student's t test or Mann-Whitney test for nonparametric comparisons. Statistical differences among more than two groups were assessed using one-way ANOVA followed by post-hoc Bonferroni correction. Results were considered statistically significant if the p-value was less than 0.05. Statistical analyses were performed using GraphPad Prism 6.

iPSC-CM RNA-sequencing statistical analyses: The gene expression differential analysis was performed using DESeq2 (v1.12.4). The genes with absolute fold change larger than 1.5 and false discovery rate less than 0.05 were designated as significantly differentially expressed between groups.

Murine RNA-sequencing statistical analyses: Differential expression testing was performed using edgeR v3.16.5¹⁶ and limma v3.30.13.¹⁷ Low level genes were removed within each condition using median log-transformed counts per gene per million mapped reads (cpm) cutoff of 0. Pearson correlation coefficients were calculated using the base R stats function cor between samples using the log counts per million (CPM) reads.

Proteomic Statistics: Protein measures were log-transformed and standardized to mean=0, standard deviation=1 within respective batches. Age- and sex-adjusted regression models were performed for quartile of protein (independent variable) versus the corrected QT (QTc) interval (dependent variable). QTc was calculated using the Bazett formula.

Disclaimer: The manuscript and its contents are confidential, intended for journal review purposes only, and not to be further disclosed.

Results

Clinical characteristics of study family

The proband of the family originally presented as a 14 year-old male with chest pain most likely due to costochondritis (proband noted as IV.9 in Family pedigree provided in **Figure S1a**). He had a history of palpitations but no syncopal episodes. His presenting ECG demonstrated a spontaneous type I Brugada pattern (**Fig 1a**). No *SCN5A* variant was identified on commercial sequencing. He was referred for an electrophysiology (EP) study for risk stratification which was a standard of care at the time and this revealed inducible polymorphic ventricular tachycardia for which he was treated with primary prevention placement of an implantable cardioverter defibrillator (ICD). A procainamide challenge to elicit the BrS pattern was not performed given his spontaneous type 1 BrS pattern. He declined participating in future research endeavors beyond genetic evaluation. Subsequent screening identified three additional family members with Brugada Syndrome, his mother (family member III.17), sister (family member IV.7), and brother (family member IV.10). The mother also displayed a spontaneous type 1 BrS pattern. There was one family member, a maternal great aunt to proband, who died suddenly at age 59 years but additional clinical history is not available (family member II.5; **Figure S1a**)

Targeted Sanger sequencing was performed in the parents and children identifying the previously reported novel, missense variant in *TBX5* that is absent in gnomAD 2.1 and gnomAD 3 (*c.G433A*; p.G145R, **Fig 1b, Figure S1a**).¹⁰ The elder sister (noted as IV.7 in pedigree in **Figure S1a**) was also screened based upon the family history and symptoms of palpitations without syncopal events. Procainamide challenge demonstrated a positive test with >2mm elevation of J point in V1 and downsloping ST

segment elevation and milder changes in V2; nonsustained polymorphic ventricular tachycardia was induced during the EP study. The youngest sibling (member IV.10 in pedigree) had many ECGs that were negative for spontaneous BrS pattern. A procainamide challenge test was negative at age 17 but a re-challenge at age 22 produced a positive test with >2mm elevation of J point in V2, consistent with the known age-related penetrance of this condition (**Fig 1c and Figure S1a**).^{18, 19}

Review of all available ECGs from variant carriers demonstrated rate corrected QT intervals (QTc) were normal (422-447 msec in the member IV.7 (sister) and 375-422 msec in member III.17 (mother)). However, we did observe evidence of abnormally long repolarization, localized to specific leads: QT inter-lead dispersion, assessed as the difference between longest and shortest QT measured in all 12 ECG leads (**Fig 1a**), was strikingly prolonged (104 and 78 msec [normal <60 msec;²⁰ pathologic in long QT syndrome >100 msec²¹]), and QTc in individual right precordial leads was as long as 521 msec. There is one family member (II.5) with sudden death at age 59 but no family history of syncope (See extended pedigree in **Figure S1a**).

TBX5-G145R causes BrS

Electrophoretic mobility shift assays showed a severe but incomplete loss of DNA binding capacity by TBX5-G145R relative to TBX5-WT and reduced transcriptional regulation in a TBX5-responsive enhancer luciferase reporter assay (**Fig 1d and 1e**). This markedly decreased function is consistent with a potential causative role in BrS in the index family. As the number of individuals within the family was insufficient to generate statistical evidence of linkage, we generated and validated three iPSC clones from the

elder sister (family member IV.7) in the kindred diagnosed with BrS ($TBX5^{G145R/WT}$) and four clones from healthy population controls (**Figure S2**). To directly test if the missense *TBX5* variant caused the BrS phenotype, we edited the *TBX5 c.G433A* missense variant back to the reference sequence in two BrS clones using RNA-guided Cas9 nuclease to generate isogenic controls (**Figure S3**). Sequencing of predicted off-target exonic regions did not identify off-target activity of Cas9 (**Table S1**).

Expression of *TBX5* in $TBX5^{G145R/WT}$ iPSC-CMs at 35 days post-cardiac induction was no different than population or isogenic controls by qPCR and RNA-sequencing (**Fig 2a**). However, total *SCN5A* transcripts, inclusive of both fetal and adult isoforms, were reduced by 79% compared to each control group by qPCR ($P<0.05$; **Fig 2a**); this result was also seen in the RNA sequencing experiments described below. In whole cell voltage-clamp experiments $TBX5^{G145R/WT}$ iPSC-CMs displayed ~50% reduced peak sodium current (-58 ± 4.9 pA/pF) compared to the control groups (population: -124 ± 8.0 ; isogenic: -133 ± 6.5) at a test voltage of -30 mV ($P<0.05$; **Summary data pooled by genotype presented in Fig 2b and 2d; individual clone data presented in Figure S4-7 and Table S4**). L-type calcium and potassium currents, inconsistently implicated in BrS pathogenesis,⁷ were not different between groups (**Figure S8-10**). Thus, $TBX5^{G145R/WT}$ cells demonstrate reduced sodium current, the electrophysiologic hallmark of BrS, attributable to reduced *SCN5A* expression. The findings of phenotype reversal in the isogenic control cells establish *TBX5-G145R* as the underlying cause.

Further arrhythmogenic behaviors in $TBX5^{G145R/WT}$ iPSC-CMs

The TBX5^{G145R/WT} cells displayed abnormalities beyond reduced peak sodium current and, as we describe here, these were also restored to wild-type behavior in genome edited cells. There was an 8.7 mV shift in the voltage ($V_{1/2}$) at which half-maximal activation (Isogenic control -42.9 ± 0.5 mV; TBX5^{G145R/WT} -34.2 ± 0.6 mV) and a 10 mV shift for inactivation (Isogenic control -88.9 ± 0.3 ; TBX5^{G145R/WT} -78.9 ± 0.3 ;

Summary data pooled by genotype presented in Fig 2e and individual clone data presented in Figure S7 and summarized in Table S4). In addition to these shifts in activation and inactivation of NaV1.5 (the channel encoded by *SCN5A*), we also observed a marked increase in a non-inactivating (“late”) component of the sodium current, I_{Na-L} , at $2.2 \pm 1\%$ of peak sodium current in TBX5^{G145R/WT} iPSC-CMs but negligible I_{Na-L} in the population and isogenic controls accounting for $0.25 \pm 0.03\%$ and $0.26 \pm 0.04\%$ of peak I_{Na} , respectively (**Fig 2c and 2f**). Treatment of TBX5^{G145R/WT} iPSC-CMs with the late sodium current blocker ranolazine (3 μ M) completely eliminated I_{Na-L} (**Fig 2c and 2f**).²²

Enhanced I_{Na-L} has been reported in a number of settings, notably as a contributor to heart failure and increased action potential duration (APD) in the congenital or drug-induced forms of the long QT syndrome.²³⁻²⁵ TBX5^{G145R/WT} iPSC-CMs showed normal resting membrane potential and action potential amplitude but did display increased APD at 90% repolarization (APD₉₀) (**Summary data pooled by genotype presented in Fig 3a-b and individual clone data presented in Figure S11 and summarized in Table S2**). We generated an additional iPSC line from the affected mother to confirm the key, unanticipated electrophysiologic abnormalities. This clone also demonstrated increased I_{Na-L} and APD prolongation (**Figure S11**). Arrhythmogenic early afterdepolarizations, delayed afterdepolarizations, and triggered action potentials were observed in 4/18 of

TBX5^{G145R/WT} iPSC-CMs with pacing at 1Hz but not in any cell (n=20) studied from either control group (**Fig 3b-3d**). Afterdepolarizations with occasional triggered action potentials were also observed in the rare spontaneously beating individual TBX5^{G145R/WT} iPSC-CMs (representative tracing in **Figure S12**). These electrophysiologic abnormalities were also abolished by 3 μ M ranolazine, further implicating enhanced I_{Na-L} as the cause of the increased APD (**Fig 3b-3d**).

Beat-to-beat variability in APD is another arrhythmogenic feature linked to I_{Na-L} .²⁶ In healthy control iPSC-CMs, Poincaré plots (APD_n vs APD_{n+1}) revealed very little beat-to-beat APD variability, whereas there was substantial variability, abolished by ranolazine, in TBX5^{G145R/WT} iPSC-CMs (**Fig 3e and 3f**).²⁷ Metrics of variability in Poincaré plots include scatter plot area, short term variability (STV), and long term variability (LTV) in APD,²⁸ and all were significantly increased in TBX5^{G145R/WT} iPSC-CMs relative to population and isogenic controls (**Table S2**). Ranolazine exposure returned the TBX5^{G145R/WT} iPSC-CM Poincaré plot parameters to control values. The APD variability did not result from alterations in calcium control as parameters of calcium handling were similar in disease and control groups (**Table S3**).

We considered the possibility that the increased I_{Na-L} and afterdepolarizations might arise as a direct result of decreased NaV1.5 abundance (*e.g.* by altered interactions with function-modifying subunits). To test this idea, we generated *SCN5A* heterozygous knockout iPSC-CMs from the isogenic control cells (TBX5^{WT/WT}; *SCN5A*^{+/-}), and found NaV1.5 levels reduced to a similar degree as in TBX5^{G145R/WT} myocytes but no increased APD variability or afterdepolarizations (**Fig 4 and Table S2**).

We further probed the impact of the single-cell arrhythmogenic phenotype in a tissue-like context²⁹ by assaying the electrical properties of spontaneously beating monolayers of iPSC-CMs using extracellular field potentials (EFPs) and the contractile properties using impedance measurements.³⁰ TBX5^{G145R/WT} and control monolayers displayed regular beating rates at 50-60 beats/min with minimal variability in the beat frequency, while EFP duration (FPD) was significantly longer in TBX5^{G145R/WT} iPSC-CMs (**Figure S13a and S13b**). Poincaré plots were similar to those seen in the single cell patch clamp experiments, with TBX5^{G145R/WT} iPSC-CM monolayers showing afterdepolarizations as well as larger STV and FPD variability, both of which were reduced by 3 μ M ranolazine (**Figure S13c-13e and Table S5**). In contrast to the dramatic differences in EFP characteristics, we observed only modest differences in impedance parameters between lines. Impedance pulse width at 30% peak height was minimally prolonged in TBX5^{G145R/WT} monolayers, consistent with the prolonged action potentials in these cells, and there was no difference in 50% peak height or 90% peak height between lines (**Figure S13f**). These data indicate that contractile function was minimally affected in TBX5^{G145R/WT} cells, in contrast to the significant changes in these parameters observed in models of cardiomyopathy³¹ and consistent with normal contractile function in individuals with BrS.

Changes in gene expression with TBX5-G145R

Holt-Oram Syndrome (HOS) is defined by septal defects and upper limb abnormalities and is caused by severe loss-of-function (LOF) variants in *TBX5*. Our family members do not have overt HOS presentation recognized prior to the

identification of the TBX5-G145R variant. Additional clinical phenotyping and family history found subtle and variably expressive thumb hypoplasia, and a single member with a ventricular septal defect (see family pedigree in **Figure S1a and S1b**). Biochemical assays demonstrated that TBX5-G145R is not a complete LOF variant, since it maintained ~3% DNA binding capacity and ~38% transcriptional activity compared to wild-type TBX5 (**Fig 1d and 1e**). In order to understand the differences in gene regulation resulting from the BrS-identified G145R variant compared to canonical HOS TBX5 haploinsufficiency, we generated isogenic iPSC lines carrying heterozygous *TBX5* frameshifting insertion or deletion (indel) variants, thereby creating an HOS iPSC-CM model ($TBX5^{-/WT}$; **Figure S14 and S15**). We performed RNA-sequencing (at least three clones each) from population controls as well as the following isogenic groups: $TBX5^{G145R/WT}$, the CRISPR-corrected $TBX5^{G145R/WT}$ group ($TBX5^{WT/WT}$), and $TBX5^{-/WT}$. Consistent with the qPCR data, the TBX5-G145R samples showed a $53 \pm 13\%$ reduction in *SCN5A* expression in the RNA-sequencing dataset (**Fig 5a**). Human iPSC-CMs express the fetal and adult isoforms of *SCN5A* which are both reduced in TBX5-G145R containing cardiomyocytes. The fetal isoform was reduced by 50% and the adult form by 70% compared to control cardiomyocytes. Sixteen other genes rarely associated with BrS including *SCN10A* and the function-modifying subunits *SCN1B*, and *SCN3B* were not differentially expressed (**Table S6**).⁵

Unsupervised hierarchical clustering of adult human ventricle-enriched genes identified a distinct gene expression signature in $TBX5^{-/WT}$ iPSC-CMs relative to $TBX5^{G145R/WT}$ iPSC-CMs, which clustered more closely with the control lines (**Figure S16a and S16b**). There was a greater reduction in *SCN5A* expression in $TBX5^{-/WT}$ iPSC-

CMs compared to TBX5^{G145R/WT} iPSC-CMs and a significant reduction in expression of *NPPA*, a previously characterized direct TBX5 target (**Fig 5a-b**).¹⁵ Functional pathway analysis of the 234 genes differentially expressed in haploinsufficient TBX5^{-/WT} iPSC-CMs compared to the TBX5^{G145R/WT} revealed enrichment for genes governing heart morphogenesis and cardiovascular development including reduced levels of cardiac transcription factors *HEY2*^{32, 33} and *ETVI*³⁴ and structural genes *MYL2* and *MB*, supporting TBX5-G145R as a hypomorphic loss-of-function variant and the known role of TBX5 in cardiogenesis (**Fig 5b, Figure S16a-c, and Table S7**).³⁵ Interestingly, *HEY2* has also been implicated as a regulator of *SCN5A* function and of the BrS phenotype.^{32, 36, 37}

The distinct effect of TBX5^{G145R/WT} on I_{Na-L} phenotypes prompted us to perform additional gene ontology analyses in order to identify other arrhythmogenic pathways beyond reduced *SCN5A* expression. Due to the hypomorphic impact of TBX5-G145R on gene expression, we expanded our analysis to include all genes with significant (adjusted p-value <0.05) and sub-threshold (>1.5-fold change in expression with an uncorrected p value < 0.05) differential expression compared to control lines as part of hypothesis generating evaluation (**Fig 5c and Table S8-S9**). This approach identified functional enrichment in genes involved with regulation of the phosphoinositol-3 kinase (PI3K) signaling pathway in TBX5^{G145R/WT} iPSC-CMs compared to control cardiomyocytes. TBX5^{G145R/WT} iPSC-CMs have reduced gene expression of multiple upstream transmembrane receptors (*PGFRA*, *TEK*, *FLT1*) or their ligands (*IGF1* and *HB-EGF*) that are activators of the PI3K cascade.

Reduced PI3K activity with resultant enhanced late sodium current has been implicated as a mechanism of arrhythmia risk in diabetes²³ or caused by exposure to QT prolonging drugs,^{25, 38} so we hypothesized that our observed cellular arrhythmia phenotypes were due to altered PI3K signaling. Phospho-specific antibodies against the PI3K targets Akt and S6 and semi-quantitative analysis by Western blot revealed a non-statistically significant trend for reduced basal phosphorylation in TBX5^{G145R/WT} iPSC-CMs compared to isogenic myocytes of 31% and 45% reduction, respectively (**Fig 5d**). To more accurately quantify PI3K activity, we utilized a more sensitive method to assess phosphorylation state by quantifying radiolabeled phosphoinositides by HPLC after tritiated-inositol labelling,³⁹ and found TBX5^{G145R/WT} iPSC-CMs had a 61% reduction in basal levels of PIP₃ (the downstream effector of PI3K signaling) compared to isogenic control myocytes ($P<0.05$; **Fig 5f**). We used Western blot analysis of Akt phosphorylation to study the effects of PI3K pathway ligands identified by pathway analysis (IGF1, VEGF, PDGF, HB-EGF, and Angiopoietin-1). There was 3-4 fold increase in Akt phosphorylation with pooled exposure to these ligands. Follow-up experiments demonstrated that this effect was attributable to PDGF alone, with minimal effects of the other ligands (**Fig 5e**). These results were confirmed by HPLC quantification of radiolabeled phosphoinositides which showed that one-hour stimulation with PDGF increased PIP₃ levels 3.4 and 3.9-fold in TBX5^{G145R/WT} and isogenic control iPSC-CMs, respectively (**Fig 5f and Figure S17**), while treatment with IGF-1 and VEGF had no effect on Akt phosphorylation or PIP₃ levels.

Electrophysiologic effects of PDGF and of the PDGF receptor antagonist crenolanib

We tested the potential of PDGF to blunt the arrhythmogenic phenotype we observed in TBX5^{G145R/WT} iPSC-CMs. As shown in **Fig 6a and 6b**, treatment with PDGF in these cells significantly reduced I_{Na-L} ($P=0.003$, **Figure S18**), shortened APD and reduced APD variability in individual iPSC-CMs; the effects were similar to those observed with intracellular perfusion with PIP3 (**Fig 6c and Table S2**).^{23, 25} The rightward voltage shifts in sodium channel activation and inactivation were also restored to the $V_{1/2}$ recorded in control myocytes at -44.3 ± 1.2 and -86.9 ± 1.4 mV ($n=9$), respectively. By contrast, treatment with IGF1 did not impact the described arrhythmia phenotypes (**Figure S19**). To test if PDGF directly blocks I_{Na-L} , we studied I_{Na-L} in HEK cells transfected with wild-type NaV1.5 or mutant F1486L that causes *SCN5A*-associated type 3 congenital long QT syndrome⁴⁰ because of enhanced I_{Na-L} : PDGF caused no change in the magnitude of I_{Na-L} in wild-type or F1486L cells (**Figure S20**). Treatment with PDGF also completely abolished afterdepolarization-triggered action potentials and resolved APD variability in isolated TBX5^{G145R/WT} iPSC-CMs (**Fig 6b and Table S2**). Additionally, PDGF exposure also reduced the EFP duration variability in TBX5^{G145R/WT} iPSC-CM monolayers (**Table S5**). The extent of this reduction was similar to that seen with the I_{Na-L} blocker ranolazine, supporting a common mechanism of increased I_{Na-L} (**Table S5**).

In heterologous expression systems, we have previously reported that the effect of PI3K on late sodium current is mediated by the α -isoform.⁴¹ We also reported that the PI3K α inhibitor A66 phenocopied the anticipated electrophysiologic phenotypes of increased late sodium current and APD prolongation in control iPSC-CMs⁴² and here we tested if chemical blockade of the PDGF pathway had a similar result. We found that the

PDGF receptor inhibitor crenolanib strikingly prolonged action potential duration in control iPSC-CMs, to >1000 msec, and this was reversed to normal duration with ranolazine exposure (**Fig 6d**). The findings were also seen in adult mouse left ventricular myocytes, where crenolanib treatment caused marked APD prolongation and afterdepolarization-triggered action potentials (**Fig 7a**).

PDGF dysregulation in developing mouse and in a human population

We addressed whether TBX5 regulation of PDGF signaling occurs in biological contexts other than TBX5^{G145R/WT} iPSC-CMs by studying established *Tbx5* null murine models. We found that in multiple developmental settings, removal of *Tbx5* caused diminished expression of genes in the PDGF axis, including *Pdgfb*, *Pdgfd*, and *Pdgfra*. We analyzed RNA-Seq data from heart tubes collected from embryonic day 9.5 (E9.5) embryos with germline deletion of *Tbx5*.^{15, 43} *Tbx5* deleted heart tubes displayed a significant 1.65-fold decrease in *Pdgfra* expression compared to littermate controls. To avoid the confounding requirement of *Tbx5* in early heart organogenesis, we also analyzed gene expression from the E12.5 left ventricle 24-hours following inducible deletion of *Tbx5* using R26R-CreERT2. We observed reduced expression of two PDGF receptors, *Pdgfra* and *Pdgfrl* (**Fig 7b**). Furthermore, upstream ingenuity pathway analysis predicted significant reduction of the PDGF-BB signaling axis (z-score -2.91, p-value=1.15E-10, rank 18/928 pathways by p-value). It has previously been shown that *Tbx5* null cardiomyocytes have APD prolongation compared to wild-type littermate controls (51-68 vs 144-188 ms).^{44, 45} These results support the role of TBX5 in regulating

the PDGF/PI3K signaling cascade in both *in vitro* human iPSC-CMs and *in vivo* murine cardiac developmental contexts.

To investigate if PDGF signaling broadly influences electrical signaling in the general human population, we directly measured plasma growth factor levels in healthy individuals in the Framingham Heart Study Offspring Cohort with ECG data available (n=1,893 individuals). There was no correlation between QT measurement and insulin and IGF-1 but there was an inverse correlation between higher plasma levels of PDGF-B and shorter QTc intervals (**Fig 8**, $P=0.0001$). These data support a common mechanism of PDGF being a modifier of cardiac repolarization as evaluated by QTc in the general population.

Disclaimer: The manuscript and its contents are confidential, intended for journal review purposes only, and not to be further disclosed.

Discussion

Correct assignment of causation to a rare genetic variant is critical to the care of affected individuals and their families and is becoming a growing problem as the use of panel-based sequencing is increasingly identifying rare variants of unknown significance. To date, the strongest evidence that a rare genetic variant causes a familial arrhythmia syndrome has come from linkage analysis, which requires large kindreds with multiple affected family members. In the absence of large kindreds, causation has sometimes been inferred by the discovery of a rare variant in a logical candidate gene and functional studies that support causation. However, this logic can be flawed, as evidence reviews have, for example, downgraded assertions of pathogenicity in some putative BrS and LQTS genes.^{7, 46, 47} Thus, stringent experimental evidence is required for variants discovered in novel genes, not established for a particular disease, as in our index case reported here. This provides an example of how the development of patient-specific iPSC-CMs represents an important new approach to address this problem. The reduced sodium current in our patient-specific iPSC-CMs compared to population controls is consistent with the known pathophysiology of BrS, but does not address whether TBX5-G145R causes or even contributes to the cellular or clinical phenotype. Another TBX5 variant (F206L) has been described in familial BrS further supporting TBX5 as potential BrS gene but our work establishes genetic causation.⁴⁸ It is the correction by gene editing of this electrophysiologic abnormality that firmly establishes G145R as the cause of the abnormality in this family and that *TBX5* is a novel BrS causative gene. However, further work is required to determine if all or only a subset of TBX5 variants increases an individual's risk of BrS or additional arrhythmias.

Transcriptional profiling in patient-derived and genetically-edited cells implicated decreased expression of a set of genes converging on PI3K signaling, and a single ligand, PDGF, rescued the defect in PI3K signaling and reversed the arrhythmogenic phenotype. These mechanisms are conserved across species as genetic deletion of *Tbx5* in mice reduced expression of multiple genes in the PDGF axis, including *Pdgfra*, and chemical inhibition of the PDGF receptor resulted in arrhythmogenic APD prolongation in both human iPSC-CMs and murine ventricular cardiomyocytes. The results of these functional studies were supported using the completely orthogonal population proteomic analysis, which identified serum PDGF levels as a modifier of human QTc, a known proxy of arrhythmia risk which is all the more remarkable since initial studies implicating perturbed PI3K signaling as an arrhythmogenic pathway studied arrhythmias due to exposure to QT-prolonging drugs.^{25, 38} These results thus define a novel genetically-defined transcriptional mechanism, culminating in decreased PI3K activity, of arrhythmia susceptibility.

Post-translation modifications of NaV1.5 by phosphorylation and nitrosylation are known modifiers of I_{Na-L} .⁴⁹ We have shown that chronic exposure to the QT prolonging agent dofetilide (previously classified as a “pure” blocker of the potassium current I_{Kr}) enhanced I_{Na-L} in Chinese hamster ovary cells expressing the cardiac sodium channel and in human iPSC-CMs through reduced PI3K activity that was rescued by intracellular delivery of PIP_3 .²⁵ In the present report we identified a novel transcriptional mechanism of disrupted regulation of upstream PI3K activators causing increased I_{Na-L} . QT prolongation is a recognized potentially fatal side effect of tyrosine kinase inhibitors (TKIs), particularly those that have off-target blockade of PDGF α -receptor.^{23, 50} Others

have shown that exposure of human iPSC-CMs to the TKIs nilotinib and vandetanib prolonged the duration of spontaneous action potentials and decreased the spontaneous beat rate,⁵⁰ and the data reported here also raise the possibility that PDGF receptor targeting therapies may carry arrhythmogenic potential. The role of PDGF in the pathogenesis of arrhythmia and contractile phenotypes continues to evolve. Phase II clinical trial safety data are unavailable for crenolanib but other PDGF inhibitors, such as midostaurin and quizartinib, are associated with QT prolongation in 11% and 5-13% of patients, respectively.⁵¹ PDGF signaling is critical in the electromechanical remodeling in sheep atrial myocyte and myofibroblast coupling.⁵² Further, the PDGF pathway has also been implicated in *FLNC* and *LMNA*-associated cardiomyopathies pathogenesis through enhanced expression of *PDGFRA* or *PDGFRB*.^{53, 54} A more complete understanding of the PDGF axis on both arrhythmic and contractile phenotypes is needed.

An additional variant in *TBX5* (p.D111Y) has been identified in family with LQTS with normal sodium current density and presence of increased late sodium current, prolonged action potential, and after depolarizations attributed to dysregulation of Ca/calmodulin kinase II δ signaling cascade.⁴⁸ There is growing evidence that demonstrates that disrupted *TBX5*-mediated transcription can result in a spectrum of cardiac manifestations to ranging from abnormal cardiac development to electrophysiologic manifestations. Our data presented in this report extend our understanding of *TBX5* biology and support the idea that the mechanism of the action potential prolongation due to *TBX5*-G145R or reduced PDGF signaling is increased I_{Na-L} secondary to reduced PI3K activity.

A limitation of this study is that we have not identified a translational direction to directly modify growth factor signaling as a therapeutic. Growth factor signaling is delicately balanced and utilizing exogenous PDGF therapeutically thus may not be feasible; for example, mouse models of exogenous PDGF-AA delivery led to atrial fibrosis and atrial fibrillation.⁵⁵ Therefore, we propose an alternative and safer approach to treating the reduced receptor tyrosine kinase signaling contributions to arrhythmia may be to target the downstream mechanism, such as increased I_{Na-L} , a known effect of ranolazine. We measured growth factor levels in plasma but these data will not precisely define the local signaling context within the functional myocardium in the healthy donor studied. Our study established an association between plasma PDGF-B and QTc and causation is inferred based upon data collected in our cell and murine model systems.

The phenotypes of increased I_{Na-L} and APD prolongation that we observed are not typical features of BrS; rather they are a recognized cause of QT interval prolongation in a range of settings, including the congenital long QT syndrome (cLQTS). As described in the “Clinical characteristics of the study family” section, the rate corrected QT interval (QTc) in subjects from whom we generated and studied iPSC-CMs was normal on multiple ECGs but did have evidence of abnormally long repolarization, localized to specific leads: QT inter-lead dispersion and QTc in individual right precordial leads as long as 521 msec. QT inter-lead dispersion has been proposed as a better predictor of arrhythmia risk than QTc itself and remains debated in the electrophysiology community.^{56, 57} Further, global electrical heterogeneity is associated with increased risk of drug induced-torsades de pointes independent of QTc interval.⁵⁸ The observation of action potential prolongation at the single cell level and QTc that is only mildly abnormal

is also compatible with the idea raised by others that iPSCs may reveal cellular phenotypes that are not uniformly translated to the whole heart, may require environmental cues, or are influenced by basal or fluctuating endocrine/paracrine signaling.⁵⁹ For example, in the case of some cardiomyopathies, cellular phenotypes are easily appreciated in iPSC-CMs while no phenotype occurs in mouse models or humans until adulthood or after stress.^{31, 60}

This report establishes a transcriptional mechanism of reduced PI3K signaling and arrhythmia risk driven by increased late sodium current. There are downstream questions the data raise that would merit further study. While we demonstrate a transcriptional relationship between TBX5 activity and PDGF activity, the presented experiments cannot differentiate from a primary (PDGFRA as a direct target of TBX) or secondary regulatory role. Human ChIP-sequencing data for TBX5 in cardiomyocytes are not currently achievable with commercially available antibodies which would provide insight into the localization of the transcription factor (mutant and wild-type) within the genome. Additionally, we observe significant prolongation of the action potential in TBX5-G145R containing iPSC-CMs while there is no phenotype on calcium handling properties. We observed normal decay of the calcium transient in our cells and this may reflect the fact that iPSC-CMs are immature relative to the cardiomyocytes in the adult human heart with calcium handling characteristics more similar to neonatal or fetal cardiomyocytes. Future studies are warranted to investigate the relationship between late sodium current and calcium handling.

Patient-directed investigation of rare genetic variation in combination with population-level validation has the potential to provide insight into underlying disease

mechanisms and risk. Even though the index family does not display clinical long QT syndrome, this family may possess increased susceptibility of drug-induced QT prolongation and the population study supports the results of the observed cellular phenotypes. In combination, this report raises the strong possibility that extracellular growth factors that modify PI3K activity may alter susceptibility to arrhythmias in diverse settings, such as heart failure or drug exposure as discussed above. The balance of PI3K and Akt in the failing heart modifies protective processes such as influencing chronic hypertrophic response,⁶¹ cardiomyocyte apoptosis,⁶² and, as demonstrated in this report, the magnitude of arrhythmogenic late sodium current, and thus represents a novel pathway for arrhythmia susceptibility and management.

Disclaimer: The manuscript and its contents are confidential, intended for journal review purposes only, and not to be further disseminated.

Acknowledgments: The Vanderbilt VANTAGE Core provided technical assistance for this work. This work was conducted in part using the resources of the Advanced Computing Center for Research and Education at Vanderbilt University, Nashville, TN. We thank Fabio Badilini and Martino Vaglio from AMPS-LLC for providing and adapting CalECG software to support QT measurements.

Disclaimer: The manuscript and its contents are confidential, intended for journal review purposes only, and not to be further disclosed.

Sources of Funding:

This work was supported by National Institutes of Health grants U19 HL65962, P50 GM115305; K.R.B. and A.T.H. were supported by NIGMS T32 GM07347 through the Vanderbilt Medical-Scientist Training Program. K.R.B. was also supported by NHLBI F30HL127962. S.P. was supported by NHLBI F30HL131179-01. A.G. is supported by NHGRI K99/R00HG010904. A.N.J. was supported by NIDDK T32DK007563, NINDS T32NS007491, and NIGMS RO1GM115892. J.D.M was supported by The Vanderbilt Faculty Research Scholars Fund and American Heart Association 15MCPRP25620006. M.D.B. was supported by K08HL145095. C.H. was supported by R01HL135129-A1. J.D.S. was supported by NIGMS T32 GM007183 and NHLBI T32 HL007381. J.D.Y. was supported by NIH R01 GM12440401. J.E.S. was supported by the Cancer ITMO of the French National Alliance for Life and Health Sciences (AVIESAN): “Plan Cancer 2014-2019”. The Vanderbilt VANTAGE Core is supported in part by CTSA Grant 5UL1 RR024975-03, the Vanderbilt Ingram Cancer Center P30 CA68485, the Vanderbilt Vision Center P30 EY08126, and NIH/NCRR G20 RR030956.

Conflict of Interest Disclosures: none

Disclaimer: The manuscript and its contents are confidential, intended for journal review purposes only, and not to be further disclosed.

Author contributions: K.R.B., T.Y., and D.M.R. conceived of and designed experiments. K.R.B., Q.S.W., P.J.K, C.C.H., E.R.B., E.P., Y.J., M.A.B., and L.S. identified and recruited study participants, generated iPSC lines, and edited iPSC genome using CRISPR/Cas9 system. K.R.B., C.C.C., A.N.J., A.M.G., and L.S biochemically characterized mutant TBX5 function. K.R.B., T.Y., S.P., K.K., D.O.K., B.C.K., and D.M.R performed, analyzed, and interpreted all electrophysiology experiments. J.E.S. performed and analyzed electrocardiographic analysis. A.T.H. and J.D.Y. performed and analyzed phosphoinositide labeling experiments. K.R.B., J.D.B., M.A.B., C.S., and Q.S. prepared samples for iPSC-CM RNA-sequencing and analyzed datasets. J.D.S. and I.P.M. performed and analyzed the murine RNA-sequencing experiments. J.D.M., A.M.G., K.R.B., M.D.B., M.J.K., D.N., R.S.V., Q.Y., R.E.G., G.P.J., B.N., M.F.M., and T.J.W. performed and analyzed plasma protein-related investigations. K.R.B. and D.M.R wrote the manuscript with input from all the authors.

Supplemental Materials

Online-only Supplemental Methods

Online-only Tables I - VIII

Online-only Figures I –XX

Disclaimer: The manuscript and its contents are confidential, intended for journal review purposes only, and not to be further disclosed.

Figure 1 Clinical and biochemical characterization of a familial Brugada syndrome-associated TBX5 variant. (a) Representative Brugada syndrome ECG pattern of affected family member with QT dispersion of >100ms. Red arrows highlight ST segment elevation in right precordial leads. (b) Sanger sequencing confirmation of hypothesized risk allele in *TBX5* c.G433A. (c) Representative positive procainamide challenge testing with J-point elevation elicited in V2. (d) Electrophoretic mobility shift assay demonstrates TBX5-G145R has reduced DNA binding capacity by 97% compared to wild-type protein. TBX5-G80R included as loss of function control variant that has no DNA binding capacity. (e) TBX5-G145R has reduced luciferase activity compared to WT which was performed in triplicate.

Disclaimer: The manuscript and its contents are confidential, intended for journal review purposes only, and not to be further disclosed.

Figure 2 Abnormal sodium channel expression and electrophysiology in TBX5^{G145R/WT} iPSC-CMs. (a) RNA levels of *TBX5* and *SCN5A* normalized to *RPL19* transcript in iPSC-CMs. In this and subsequent figures, data from TBX5^{G145R/WT} cells are indicated in red and from TBX5^{G145R/WT} cells with G145R edited back to G in blue. Summary data of 4-6 cardiomyocyte differentiations for four independent clones per group. (b) Representative whole cell voltage clamp recordings at voltage steps from -100 to 20 mV in 10 mV increments. Inset voltage clamp protocol. Summary data presented in panel e. (c) Representative sodium current recordings highlighting late current. Inset voltage clamp protocol. (d) Peak sodium current density plotted against test voltages (Population control (ctrl): $n=14$; TBX5^{G145R/WT}: $n=16$; Isogenic ctrl: $n=9$). (e) Voltage-dependence of steady-state inactivation and activation. (f) Quantification of late sodium current. Ranolazine treatment: 3 μ M. (Population control (ctrl): $n=10$; TBX5^{G145R/WT}: $n=10$; Isogenic ctrl: $n=7$). All summarized data displayed as mean \pm S.E.M. Means were compared using one-way ANOVA followed by post-hoc Bonferroni correction.

Disclaimer: The manuscript and its content are confidential, intended for journal review only, and not to be further disclosed.

Figure 3 Arrhythmogenic changes in cardiac action potential in TBX5^{G145R/WT} iPSC-CMs. (a) Representative action potential traces recorded at 1 Hz. (b) Averaged resting membrane potential (RMP), action potential amplitude (APA), action potential duration at 50% (APD₅₀) and 90% repolarization (APD₉₀). (Population control (ctrl): *n*=13; TBX5^{G145R/WT}: *n*=21; Isogenic ctrl: *n*=16). * indicates *P*<0.05 compared to TBX5^{G145R/WT} iPSC-CMs. (c) Early afterdepolarizations and delayed afterdepolarizations after a triggered beat (TB) (d) were observed in TBX5^{G145R/WT} iPSC-CMs but not in population or isogenic control cells (arrows). (e) Superimposed action potentials from single iPSC-CMs demonstrate APD variability in the TBX5-G145R cell. (f) Poincaré plots comparing the APD of each beat (N APD₉₀) to the APD (N+1 APD₉₀) of the subsequent beat. Dashed ellipse represents scatter area. All summarized data displayed as mean±S.E.M. Ranolazine treatment: 3μM in TBX5^{G145R/WT}: *n*=21. Means were compared using one-way ANOVA followed by post-hoc Bonferroni correction. See Table S2 for summary data including number of cells studied per group.

Disclaimer: The manuscript and its content are confidential, intended for journal review purposes only, and not to be further disclosed.

Figure 4 Heterozygous SCN5A knockout iPSC-CM arrhythmia models generation and characterization. (a) Schematic of genome editing result using CRISPR/Cas9 in patient-derived iPSCs to generation loss of function *SCN5A* Brugada syndrome model. Modified nucleotide variants and amino acids indicated as red text. (b) Representative superimposed action potentials recorded from isogenic TBX5^{WT/WT}; SCN5A^{-/WT}. Summary data provided in Table S2, *n*=4.

Disclaimer: The manuscript and its contents are confidential, intended for journal review purposes only, and not to be further disclosed.

Figure 5 Reduced phosphoinositol-3 kinase activity in TBX5^{G145R/WT} iPSC-CMs (a) *SCN5A* expression measured by RNA-sequencing for each study group normalized to population control. See methods for experimental details. (b) Volcano plot of differentially expressed genes in TBX5^{-/WT} compared to TBX5^{G145R/WT} iPSC-CMs. Red dots highlight genes implicated in heart development biologic pathway. (c) Volcano plot of differentially expressed genes in TBX5^{G145R/WT} compared to population control iPSC-CMs. Red dots highlight genes implicated in regulation of phosphoinositol-3 kinase signaling biologic pathway. (d) Quantification of Western blot analysis using phospho-specific antibodies of known phosphoinositol-3 kinase targets S6 and Akt normalized to total protein of each target. *n* = 3 biologic replicates per group (e) Western blot analysis for phosphorylation of Akt after 2-hour incubation with vehicle or ligands in combination or individually. Ligands are those identified by gene ontology with reduced expression by RNA-sequencing. (f) Representative HPLC traces and summary data of inositol species quantification. *indicates *P*<0.05

Disclaimer: The manuscript and its content are confidential, intended for journal review only, and not to be further disclosed.

Figure 6 Reduced phosphoinositol-3 kinase activity promotes arrhythmias iPSC-CMs (a) Representative I_{Na} traces with repetitive stimulation with acute treatment with PDGF in TBX5^{G145R/WT} iPSC-CM. (b) Representative superimposed action potentials recorded from TBX5^{G145R/WT} iPSC-CM treated with vehicle or PDGF for 2-hours. Summary data provided in Table S2. (c) Representative action potential recording over time with intracellular PIP₃ treatment in TBX5^{G145R/WT} iPSC-CMs. (d) Representative APs recorded from control iPSC-CMs at baseline, after 2-hour crenolanib treatment, and crenolanib + ranolazine treatment. All summarized data displayed as mean±S.E.M. Means were compared using one-way ANOVA followed by post-hoc Bonferroni correction.

Disclaimer: The manuscript and its contents are confidential, intended for journal review purposes only, and not to be further disclosed.

Figure 7 TBX PDGF phenotypes conserved in mouse cardiomyocytes

(a) Representative mouse ventricular cardiomyocyte (CM) action potentials recorded at pacing rate of 5 Hz and (e) 0.1Hz after 2 hour treatment with vehicle or 100 nM crenolanib. Triggered action potentials (TA) were observed in Crenolanib treated cells paced at 0.1Hz (b) Pearson correlation and hierarchical clustering of biological replicates for the transcriptional profiling of mouse embryonic left ventricle 24-hours after conditional knockout in *Tbx5*^{flox/flox} and controls (left). Differential expression testing of transcriptional profiles with *Pdgfra* and *Pdgfrl* (bold) and members of the PDGF-BB signaling axis that predict inhibition (blue), activation (red), or affected (black) by conditional knockout of *Tbx5* (right).

Disclaimer: The manuscript and its contents are confidential, intended for journal review purposes only, and not to be further disclosed.

Figure 8 Altered levels of plasma PDGF is associated with QT interval in the general population (a) Mean QTc +/- SE plotted for quartiles of log-transformed measured plasma PDGF beta in healthy individuals.

Disclaimer: The manuscript and its contents are confidential, intended for journal review purposes only, and not to be further disclosed.

References

1. Liang P, Sallam K, Wu H, Li Y, Itzhaki I, Garg P, Zhang Y, Vermglinchan V, Lan F, Gu M, Gong T, Zhuge Y, He C, Ebert AD, Sanchez-Freire V, Churko J, Hu S, Sharma A, Lam CK, Scheinman MM, Bers DM and Wu JC. Patient-Specific and Genome-Edited Induced Pluripotent Stem Cell-Derived Cardiomyocytes Elucidate Single-Cell Phenotype of Brugada Syndrome. *Journal of the American College of Cardiology*. 2016;68:2086-2096.
2. Karakikes I, Stillitano F, Nonnenmacher M, Tzimas C, Sanoudou D, Termglinchan V, Kong CW, Rushing S, Hansen J, Ceholski D, Kolokathis F, Kremastinos D, Katoulis A, Ren L, Cohen N, Gho JM, Tsiapras D, Vink A, Wu JC, Asselbergs FW, Li RA, Hulot JS, Kranias EG and Hajjar RJ. Correction of human phospholamban R14del mutation associated with cardiomyopathy using targeted nucleases and combination therapy. *Nature communications*. 2015;6:6955.
3. Brugada P and Brugada J. Right bundle branch block, persistent ST segment elevation and sudden cardiac death: a distinct clinical and electrocardiographic syndrome. A multicenter report. *Journal of the American College of Cardiology*. 1992;20:1391-6.
4. Brugada J, Brugada R and Brugada P. Right Bundle-Branch Block and ST-Segment Elevation in Leads V1 Through V3 : A Marker for Sudden Death in Patients Without Demonstrable Structural Heart Disease. *Circulation*. 1998;97:457-460.
5. Nielsen MW, Holst AG, Olesen SP and Olesen MS. The genetic component of Brugada syndrome. *Frontiers in physiology*. 2013;4:179.
6. Hoshi M, Du XX, Shinlapawittayatorn K, Liu H, Chai S, Wan X, Ficker E and Deschenes I. Brugada syndrome disease phenotype explained in apparently benign sodium channel mutations. *Circulation Cardiovascular genetics*. 2014;7:123-31.
7. Hosseini SM, Kim R, Udupa S, Costain G, Jobling R, Liston E, Jamal SM, Szybowska M, Morel CF, Bowdin S, Garcia J, Care M, Sturm AC, Novelli V, Ackerman MJ, Ware JS, Hershberger RE, Wilde AAM, Gollob MH and National Institutes of Health Clinical Genome Resource C. Reappraisal of Reported Genes for Sudden Arrhythmic Death. *Circulation*. 2018;138:1195-1205.
8. Kapplinger JD, Giudicessi JR, Ye D, Tester DJ, Callis TE, Valdivia CR, Makielski JC, Wilde AA and Ackerman MJ. Enhanced Classification of Brugada Syndrome-Associated and Long-QT Syndrome-Associated Genetic Variants in the SCN5A-Encoded Na(v)1.5 Cardiac Sodium Channel. *Circulation Cardiovascular genetics*. 2015;8:582-95.
9. Chen Q, Kirsch GE, Zhang D, Brugada R, Brugada J, Brugada P, Potenza D, Moya A, Borggrefe M, Breithardt G, Ortiz-Lopez R, Wang Z, Antzelevitch C, O'Brien RE, Schulze-Bahr E, Keating MT, Towbin JA and Wang Q. Genetic basis and molecular mechanism for idiopathic ventricular fibrillation. *Nature*. 1998;392:293-6.
10. Behr ER, Savio-Galimberti E, Barc J, Holst AG, Petropoulou E, Prins BP, Jabbari J, Torchio M, Berthet M, Mizusawa Y, Yang T, Nannenberg EA, Dagradi F, Weeke P, Bastiaenan R, Ackerman MJ, Haunso S, Leenhardt A, Kaab S, Probst V, Redon R, Sharma S, Wilde A, Tfelt-Hansen J, Schwartz P, Roden DM, Bezzina CR, Olesen M, Darbar D, Guicheney P, Crotti L, Consortium UK and Jamshidi Y. Role of common and rare variants in SCN10A: results from the Brugada syndrome QRS locus gene discovery collaborative study. *Cardiovascular research*. 2015;106:520-9.

11. van den Boogaard M, Wong LY, Tessadori F, Bakker ML, Dreizehnter LK, Wakker V, Bezzina CR, t Hoen PA, Bakkers J, Barnett P and Christoffels VM. Genetic variation in T-box binding element functionally affects SCN5A/SCN10A enhancer. *The Journal of clinical investigation*. 2012;122:2519-30.
12. Sotoodehnia N, Isaacs A, de Bakker PI, Dorr M, Newton-Cheh C, Nolte IM, van der Harst P, Muller M, Eijgelsheim M, Alonso A, Hicks AA, Padmanabhan S, Hayward C, Smith AV, Polasek O, Giovannone S, Fu J, Magnani JW, Marciante KD, Pfeufer A, Gharib SA, Teumer A, Li M, Bis JC, Rivadeneira F, Aspelund T, Kottgen A, Johnson T, Rice K, Sie MP, Wang YA, Klopp N, Fuchsberger C, Wild SH, Mateo Leach I, Estrada K, Volker U, Wright AF, Asselbergs FW, Qu J, Chakravarti A, Sinner MF, Kors JA, Petersmann A, Harris TB, Soliman EZ, Munroe PB, Psaty BM, Oostra BA, Cupples LA, Perz S, de Boer RA, Uitterlinden AG, Volzke H, Spector TD, Liu FY, Boerwinkle E, Dominiczak AF, Rotter JI, van Herpen G, Levy D, Wichmann HE, van Gilst WH, Wittteman JC, Kroemer HK, Kao WH, Heckbert SR, Meitinger T, Hofman A, Campbell H, Folsom AR, van Veldhuisen DJ, Schwienbacher C, O'Donnell CJ, Volpato CB, Caulfield MJ, Connell JM, Launer L, Lu X, Franke L, Fehrmann RS, te Meerman G, Groen HJ, Weersma RK, van den Berg LH, Wijmenga C, Ophoff RA, Navis G, Rudan I, Snieder H, Wilson JF, Pramstaller PP, Siscovick DS, Wang TJ, Gudnason V, van Duijn CM, Felix SB, Fishman GI, Jamshidi Y, Stricker BH, Samani NJ, Kaab S and Arking DE. Common variants in 22 loci are associated with QRS duration and cardiac ventricular conduction. *Nature genetics*. 2010;42:1068-76.
13. Basson CT, Huang T, Lin RC, Bachinsky DR, Weremowicz S, Vaglio A, Bruzzone R, Quadrelli R, Lerone M, Romeo G, Silengo M, Pereira A, Krieger J, Mesquita SF, Kamisago M, Morton CC, Pierpont ME, Muller CW, Seidman JG and Seidman CE. Different TBX5 interactions in heart and limb defined by Holt-Oram syndrome mutations. *Proceedings of the National Academy of Sciences of the United States of America*. 1999;96:2919-24.
14. Linhares VL, Almeida NA, Menezes DC, Elliott DA, Lai D, Beyer EC, Campos de Carvalho AC and Costa MW. Transcriptional regulation of the murine Connexin40 promoter by cardiac factors Nkx2-5, GATA4 and Tbx5. *Cardiovascular research*. 2004;64:402-11.
15. Bruneau BG, Nemer G, Schmitt JP, Charron F, Robitaille L, Caron S, Conner DA, Gessler M, Nemer M, Seidman CE and Seidman JG. A murine model of Holt-Oram syndrome defines roles of the T-box transcription factor Tbx5 in cardiogenesis and disease. *Cell*. 2001;106:709-21.
16. Robinson MD, McCarthy DJ and Smyth GK. edgeR: a Bioconductor package for differential expression analysis of digital gene expression data. *Bioinformatics*. 2010;26:139-40.
17. Ritchie ME, Phipson B, Wu D, Hu Y, Law CW, Shi W and Smyth GK. limma powers differential expression analyses for RNA-sequencing and microarray studies. *Nucleic acids research*. 2015;43:e47.
18. Conte G and Brugada P. The challenges of performing ajmaline challenge in children with suspected Brugada syndrome. *Open Heart*. 2014;1:e000031.
19. Priori SG and Blomstrom-Lundqvist C. 2015 European Society of Cardiology Guidelines for the management of patients with ventricular arrhythmias and the

- prevention of sudden cardiac death summarized by co-chairs. *Eur Heart J*. 2015;36:2757-9.
20. Hii JT, Wyse DG, Gillis AM, Duff HJ, Solylo MA and Mitchell LB. Precordial QT interval dispersion as a marker of torsade de pointes. Disparate effects of class Ia antiarrhythmic drugs and amiodarone. *Circulation*. 1992;86:1376-1382.
 21. Priori SG, Napolitano C, Diehl L and Schwartz PJ. Dispersion of the QT interval. A marker of therapeutic efficacy in the idiopathic long QT syndrome. *Circulation*. 1994;89:1681-9.
 22. Sokolov S, Peters CH, Rajamani S and Ruben PC. Proton-dependent inhibition of the cardiac sodium channel Nav1.5 by ranolazine. *Frontiers in pharmacology*. 2013;4:78.
 23. Lu Z, Jiang YP, Wu CY, Ballou LM, Liu S, Carpenter ES, Rosen MR, Cohen IS and Lin RZ. Increased persistent sodium current due to decreased PI3K signaling contributes to QT prolongation in the diabetic heart. *Diabetes*. 2013;62:4257-65.
 24. Makielski JC. Late sodium current: A mechanism for angina, heart failure, and arrhythmia. *Trends in cardiovascular medicine*. 2016;26:115-22.
 25. Yang T, Chun YW, Stroud DM, Mosley JD, Knollmann BC, Hong C and Roden DM. Screening for acute IKr block is insufficient to detect torsades de pointes liability: role of late sodium current. *Circulation*. 2014;130:224-34.
 26. Thomsen MB, Verduyn SC, Stengl M, Beekman JD, de Pater G, van Opstal J, Volders PG and Vos MA. Increased short-term variability of repolarization predicts d-sotalol-induced torsades de pointes in dogs. *Circulation*. 2004;110:2453-9.
 27. Kaneko T, Nomura F, Hamada T, Abe Y, Takamori H, Sakakura T, Takasuna K, Sanbuissho A, Hyllner J, Sartipy P and Yasuda K. On-chip in vitro cell-network pre-clinical cardiac toxicity using spatiotemporal human cardiomyocyte measurement on a chip. *Scientific reports*. 2014;4:4670.
 28. Kamen PW and Tonkin AM. Application of the Poincare plot to heart rate variability: a new measure of functional status in heart failure. *Australian and New Zealand journal of medicine*. 1995;25:18-26.
 29. Pueyo E, Corrias A, Virag L, Jost N, Szel T, Varro A, Szentandrassy N, Nanasi PP, Burrage K and Rodriguez B. A multiscale investigation of repolarization variability and its role in cardiac arrhythmogenesis. *Biophysical journal*. 2011;101:2892-902.
 30. Doerr L, Thomas U, Guinot DR, Bot CT, Stoelzle-Feix S, Beckler M, George M and Fertig N. New easy-to-use hybrid system for extracellular potential and impedance recordings. *Journal of laboratory automation*. 2015;20:175-88.
 31. Wang L, Kim K, Parikh S, Cadar AG, Bersell KR, He H, Pinto JR, Kryshtal DO and Knollmann BC. Hypertrophic cardiomyopathy-linked mutation in troponin T causes myofibrillar disarray and pro-arrhythmic action potential changes in human iPSC cardiomyocytes. *Journal of molecular and cellular cardiology*. 2017;114:320-327.
 32. Veerman CC, Podliesna S, Tadros R, Lodder EM, Mengarelli I, de Jonge B, Beekman L, Barc J, Wilders R, Wilde AAM, Boukens BJ, Coronel R, Verkerk AO, Remme CA and Bezzina CR. The Brugada Syndrome Susceptibility Gene HEY2 Modulates Cardiac Transmural Ion Channel Patterning and Electrical Heterogeneity. *Circ Res*. 2017;121:537-548.
 33. van den Boogaard M, Smemo S, Burnicka-Turek O, Arnolds DE, van de Werken HJ, Klous P, McKean D, Muehlschlegel JD, Moosmann J, Toka O, Yang XH, Koopmann TT, Adriaens ME, Bezzina CR, de Laat W, Seidman C, Seidman JG, Christoffels VM,

- Nobrega MA, Barnett P and Moskowitz IP. A common genetic variant within SCN10A modulates cardiac SCN5A expression. *The Journal of clinical investigation*. 2014;124:1844-52.
34. Shekhar A, Lin X, Liu FY, Zhang J, Mo H, Bastarache L, Denny JC, Cox NJ, Delmar M, Roden DM, Fishman GI and Park DS. Transcription factor ETV1 is essential for rapid conduction in the heart. *The Journal of clinical investigation*. 2016;126:4444-4459.
35. Ang YS, Rivas RN, Ribeiro AJ, Srivas R, Rivera J, Stone NR, Pratt K, Mohamed TM, Fu JD, Spencer CI, Tippens ND, Li M, Narasimha A, Radzinsky E, Moon-Grady AJ, Yu H, Pruitt BL, Snyder MP and Srivastava D. Disease Model of GATA4 Mutation Reveals Transcription Factor Cooperativity in Human Cardiogenesis. *Cell*. 2016;167:1734-1749.e22.
36. Bezzina CR, Barc J, Mizusawa Y, Remme CA, Gourraud JB, Simonet F, Verkerk AO, Schwartz PJ, Crotti L, Dagradi F, Guicheney P, Fressart V, Leenhardt A, Antzelevitch C, Bartkowiak S, Borggreffe M, Schimpf R, Schulze-Bahr E, Zumhagen S, Behr ER, Bastiaenen R, Tfelt-Hansen J, Olesen MS, Kaab S, Beckmann BM, Weeke P, Watanabe H, Endo N, Minamino T, Horie M, Ohno S, Hasegawa K, Makita N, Nogami A, Shimizu W, Aiba T, Froguel P, Balkau B, Lantieri O, Torchio M, Wiese C, Weber D, Wolswinkel R, Coronel R, Boukens BJ, Bezieau S, Charpentier E, Chatel S, Despres A, Gros F, Kyndt F, Lecoq S, Lindenbaum P, Portero V, Violleau J, Gessler M, Tan HL, Roden DM, Christoffels VM, Le Marec H, Wilde AA, Probst V, Schott JJ, Dina C and Redon R. Common variants at SCN5A-SCN10A and HEY2 are associated with Brugada syndrome, a rare disease with high risk of sudden cardiac death. *Nature genetics*. 2013;45:1044-9.
37. Makarawate P, Glinge C, Khongphatthanayothin A, Walsh R, Mauleekoonphairoj J, Amnueypol M, Prechawat S, Wongcharoen W, Krittayaphong R, Anannab A, Lichtner P, Meitinger T, Tjong FVY, Lieve KVV, Amin AS, Sahasatas D, Ngarmukos T, Wichadakul D, Payungporn S, Sutjaporn B, Wandee P, Poovorawan Y, Tfelt-Hansen J, Tanck MWT, Tadros R, Wilde AAM, Bezzina CR, Veerakul G and Nademanee K. Common and rare susceptibility genetic variants predisposing to Brugada syndrome in Thailand. *Heart Rhythm*. 2020;17:2145-2153.
38. Lu Z, Wu CY, Jiang YP, Ballou LM, Clausen C, Cohen IS and Lin RZ. Suppression of phosphoinositide 3-kinase signaling and alteration of multiple ion currents in drug-induced long QT syndrome. *Science translational medicine*. 2012;4:131ra50.
39. Hale AT CB, York JD. Metabolic Labeling of Inositol Phosphates and Phosphatidylinositols in Yeast and Mammalian Cells. *Methods in mol biol*. 2018;in press.
40. Wang DW, Desai RR, Crotti L, Arnestad M, Insolia R, Pedrazzini M, Ferrandi C, Vege A, Rognum T, Schwartz PJ and George AL, Jr. Cardiac sodium channel dysfunction in sudden infant death syndrome. *Circulation*. 2007;115:368-76.
41. Yang T HC, Roden DM. Inhibition of the α -subunit of PI3 kinase increases late sodium current (INa-L) and generates arrhythmias. *Heart Rhythm*. 2015;12:5S:S150.
42. Yang T, Meoli DF, Moslehi J and Roden DM. Inhibition of the alpha-Subunit of Phosphoinositide 3-Kinase in Heart Increases Late Sodium Current and Is Arrhythmogenic. *J Pharmacol Exp Ther*. 2018;365:460-466.

43. Waldron L, Steimle JD, Greco TM, Gomez NC, Dorr KM, Kweon J, Temple B, Yang XH, Wilczewski CM, Davis IJ, Cristea IM, Moskowitz IP and Conlon FL. The Cardiac TBX5 Interactome Reveals a Chromatin Remodeling Network Essential for Cardiac Septation. *Developmental cell*. 2016;36:262-75.
44. Dai W, Laforest B, Tyan L, Shen KM, Nadadur RD, Alvarado FJ, Mazurek SR, Lazarevic S, Gadek M, Wang Y, Li Y, Valdivia HH, Shen L, Broman MT, Moskowitz IP and Weber CR. A calcium transport mechanism for atrial fibrillation in Tbx5-mutant mice. *Elife*. 2019;8.
45. Nadadur RD, Broman MT, Boukens B, Mazurek SR, Yang X, van den Boogaard M, Bekeny J, Gadek M, Ward T, Zhang M, Qiao Y, Martin JF, Seidman CE, Seidman J, Christoffels V, Efimov IR, McNally EM, Weber CR and Moskowitz IP. Pitx2 modulates a Tbx5-dependent gene regulatory network to maintain atrial rhythm. *Science translational medicine*. 2016;8:354ra115.
46. Adler A, Novelli V, Amin AS, Abiusi E, Care M, Nannenber EA, Feilotter H, Amenta S, Mazza D, Bikker H, Sturm AC, Garcia J, Ackerman MJ, Hershberger RE, Perez MV, Zareba W, Ware JS, Wilde AAM and Gollob MH. An International, Multicentered, Evidence-Based Reappraisal of Genes Reported to Cause Congenital Long QT Syndrome. *Circulation*. 2020;141:418-428.
47. Roberts JD, Krahn AD, Ackerman MJ, Rohatgi RK, Moss AJ, Nazer B, Tadros R, Gerull B, Sanatani S, Wijeyeratne YD, Baruteau AE, Muir AR, Pang B, Cadrin-Tourigny J, Talajic M, Rivard L, Tester DJ, Liu T, Whitman IR, Wojciak J, Conacher S, Gula LJ, Leong-Sit P, Manlucu J, Green MS, Hamilton R, Healey JS, Lopes CM, Behr ER, Wilde AA, Gollob MH and Scheinman MM. Loss-of-Function KCNE2 Variants: True Monogenic Culprits of Long-QT Syndrome or Proarrhythmic Variants Requiring Secondary Provocation? *Circ Arrhythm Electrophysiol*. 2017;10.
48. Nieto-Marín P, Tinaquero D, Utrilla RG, Cebrián J, González-Guerra A, Crespo-García T, Cámara-Checa A, Rubio-Alarcón M, Dago M, Alfayate S, Filgueiras-Rama D, Peinado R, López-Sendón JL, Jalife J, Tamargo J, Bernal JA, Caballero R and Delpón E. Tbx5 variants disrupt Nav1.5 function differently in patients diagnosed with Brugada or Long QT Syndrome. *Cardiovascular research*. 2022;118:1046-1060.
49. Herren AW, Bers DM and Grandi E. Post-translational modifications of the cardiac Na channel: contribution of CaMKII-dependent phosphorylation to acquired arrhythmias. *Am J Physiol Heart Circ Physiol*. 2013;305:H431-45.
50. Sharma A, Burridge PW, McKeithan WL, Serrano R, Shukla P, Sayed N, Churko JM, Kitani T, Wu H, Holmstrom A, Matsa E, Zhang Y, Kumar A, Fan AC, Del Alamo JC, Wu SM, Moslehi JJ, Mercola M and Wu JC. High-throughput screening of tyrosine kinase inhibitor cardiotoxicity with human induced pluripotent stem cells. *Science translational medicine*. 2017;9.
51. Novatcheva ED, Anouty Y, Saunders I, Mangan JK and Goodman AM. FMS-Like Tyrosine Kinase 3 Inhibitors for the Treatment of Acute Myeloid Leukemia. *Clin Lymphoma Myeloma Leuk*. 2022;22:e161-e184.
52. Musa H, Kaur K, O'Connell R, Klos M, Guerrero-Serna G, Avula UM, Herron TJ, Kalifa J, Anumonwo JM and Jalife J. Inhibition of platelet-derived growth factor-AB signaling prevents electromechanical remodeling of adult atrial myocytes that contact myofibroblasts. *Heart Rhythm*. 2013;10:1044-51.

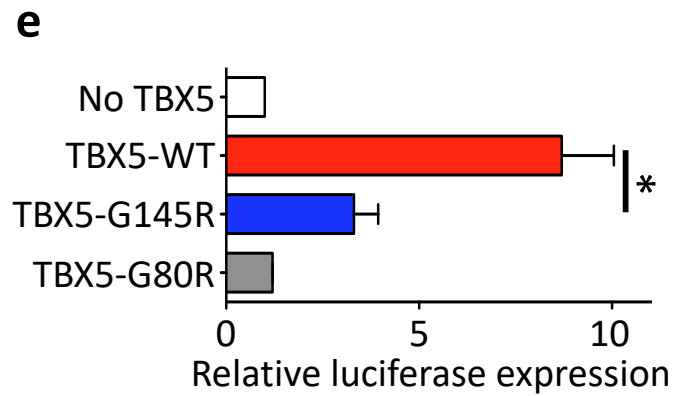
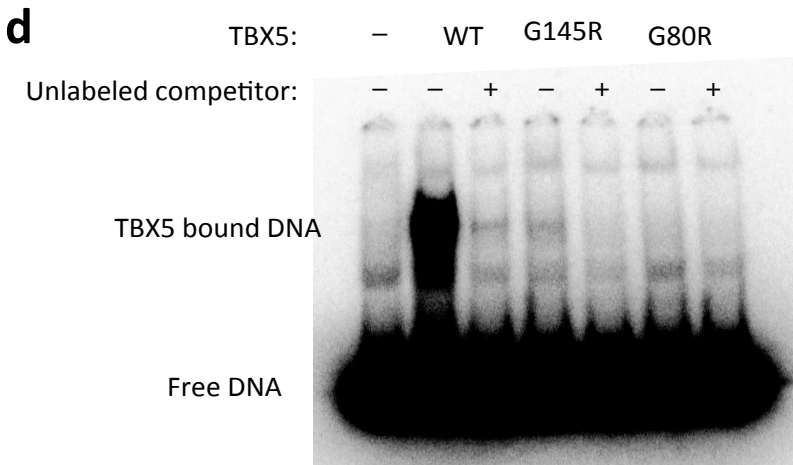
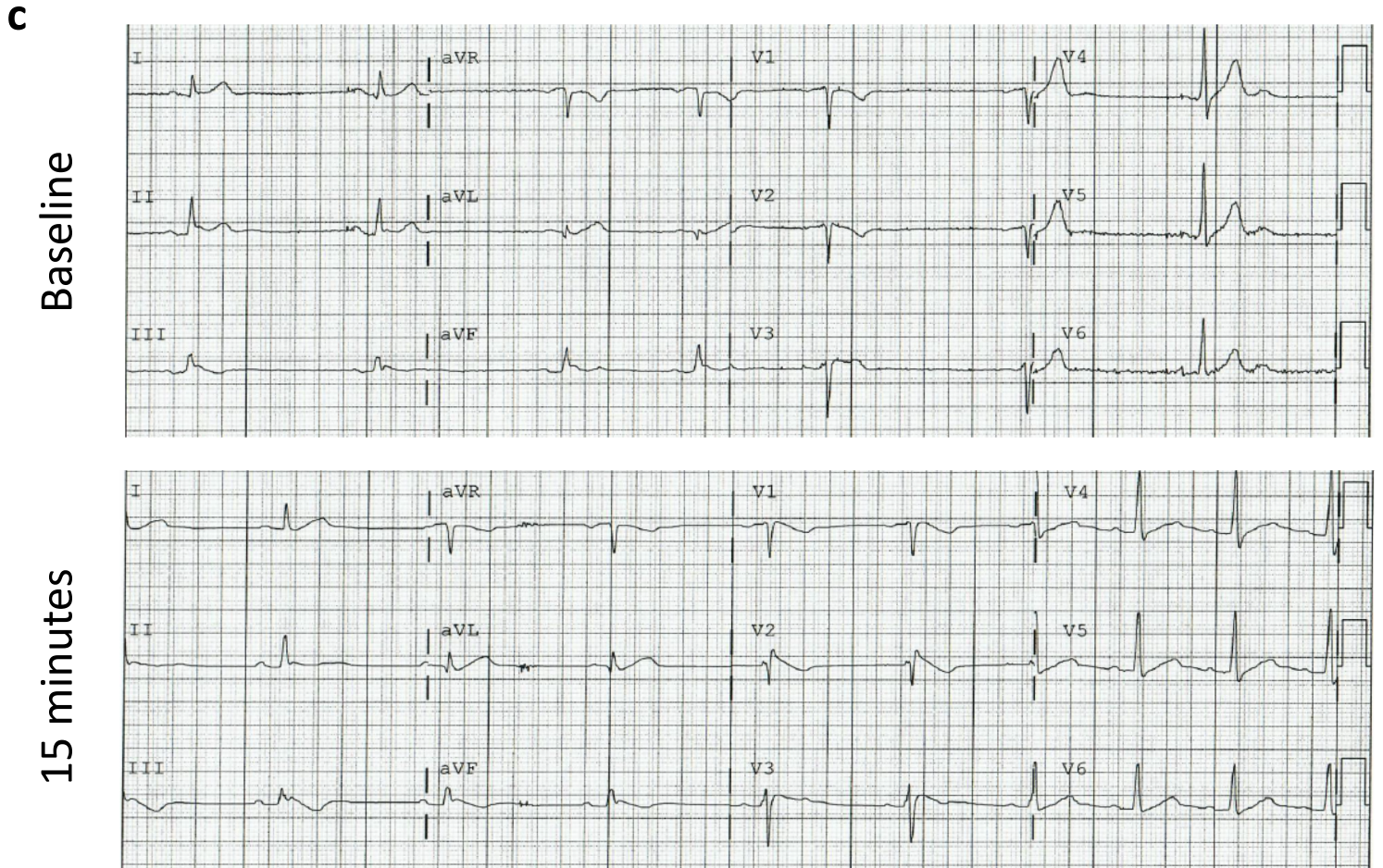
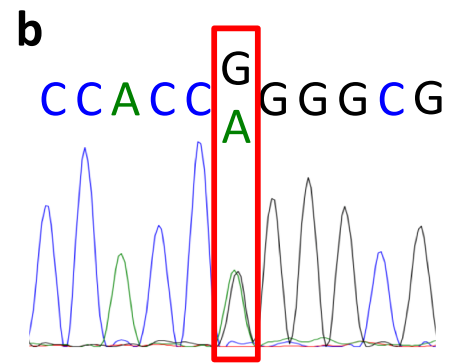
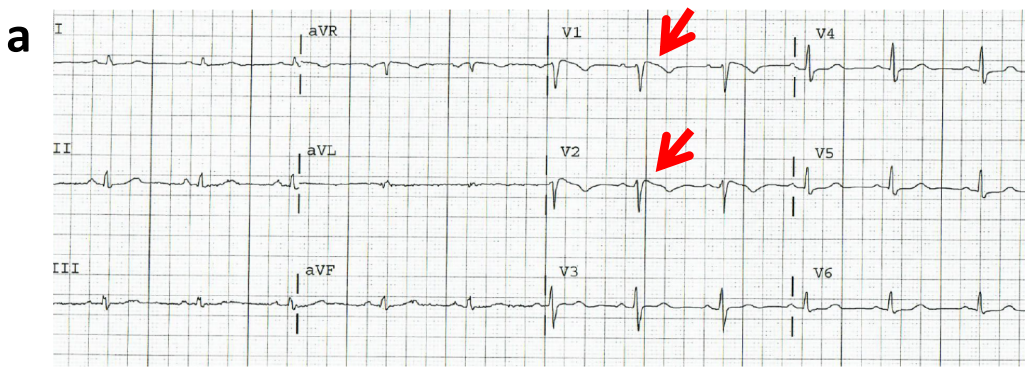
53. Chen SN, Lam CK, Wan YW, Gao S, Malak OA, Zhao SR, Lombardi R, Ambardekar AV, Bristow MR, Cleveland J, Gigli M, Sinagra G, Graw S, Taylor MRG, Wu JC and Mestroni L. Activation of PDGFRA signaling contributes to filamin C-related arrhythmic cardiomyopathy. *Sci Adv.* 2022;8:eabk0052.
54. Lee J, Termglinchan V, Diecke S, Itzhaki I, Lam CK, Garg P, Lau E, Greenhaw M, Seeger T, Wu H, Zhang JZ, Chen X, Gil IP, Ameen M, Sallam K, Rhee JW, Churko JM, Chaudhary R, Chour T, Wang PJ, Snyder MP, Chang HY, Karakikes I and Wu JC. Activation of PDGF pathway links LMNA mutation to dilated cardiomyopathy. *Nature.* 2019;572:335-340.
55. Liao CH, Akazawa H, Tamagawa M, Ito K, Yasuda N, Kudo Y, Yamamoto R, Ozasa Y, Fujimoto M, Wang P, Nakauchi H, Nakaya H and Komuro I. Cardiac mast cells cause atrial fibrillation through PDGF-A-mediated fibrosis in pressure-overloaded mouse hearts. *The Journal of clinical investigation.* 2010;120:242-53.
56. Malik M and Batchvarov VN. Measurement, interpretation and clinical potential of QT dispersion. *J Am Coll Cardiol.* 2000;36:1749-1766.
57. Galinier M, Vialette JC, Fourcade J, Cabrol P, Dongay B, Massabuau P, Boveda S, Doazan JP, Fauvel JM and Bounhoure JP. QT interval dispersion as a predictor of arrhythmic events in congestive heart failure. Importance of aetiology. *Eur Heart J.* 1998;19:1054-62.
58. Stabenau HF, Shen C, Zimetbaum P, Buxton AE, Tereshchenko LG and Waks JW. Global electrical heterogeneity associated with drug-induced torsades de pointes. *Heart Rhythm.* 2021;18:57-62.
59. Merkle FT and Eggan K. Modeling human disease with pluripotent stem cells: from genome association to function. *Cell stem cell.* 2013;12:656-68.
60. Hinson JT, Chopra A, Nafissi N, Polacheck WJ, Benson CC, Swist S, Gorham J, Yang L, Schafer S, Sheng CC, Haghighi A, Homsy J, Hubner N, Church G, Cook SA, Linke WA, Chen CS, Seidman JG and Seidman CE. HEART DISEASE. Titin mutations in iPS cells define sarcomere insufficiency as a cause of dilated cardiomyopathy. *Science (New York, NY).* 2015;349:982-6.
61. Haq S, Choukroun G, Lim H, Tymitz KM, del Monte F, Gwathmey J, Grazette L, Michael A, Hajjar R, Force T and Molkenstein JD. Differential activation of signal transduction pathways in human hearts with hypertrophy versus advanced heart failure. *Circulation.* 2001;103:670-7.
62. Matsui T and Rosenzweig A. Convergent signal transduction pathways controlling cardiomyocyte survival and function: the role of PI 3-kinase and Akt. *Journal of molecular and cellular cardiology.* 2005;38:63-71.
63. Ghosh TK, Packham EA, Bonser AJ, Robinson TE, Cross SJ and Brook JD. Characterization of the TBX5 binding site and analysis of mutations that cause Holt-Oram syndrome. *Hum Mol Genet.* 2001;10:1983-1994.
64. Ghosh TK, Song FF, Packham EA, Buxton S, Robinson TE, Ronksley J, Self T, Bonser AJ and Brook JD. Physical interaction between TBX5 and MEF2C is required for early heart development. *Molecular and cellular biology.* 2009;29:2205-18.
65. Ran FA, Hsu PD, Wright J, Agarwala V, Scott DA and Zhang F. Genome engineering using the CRISPR-Cas9 system. *Nature protocols.* 2013;8:2281-308.
66. Antoons G, Oros A, Beekman JD, Engelen MA, Houtman MJ, Belardinelli L, Stengl M and Vos MA. Late na^{+} current inhibition by ranolazine reduces torsades de

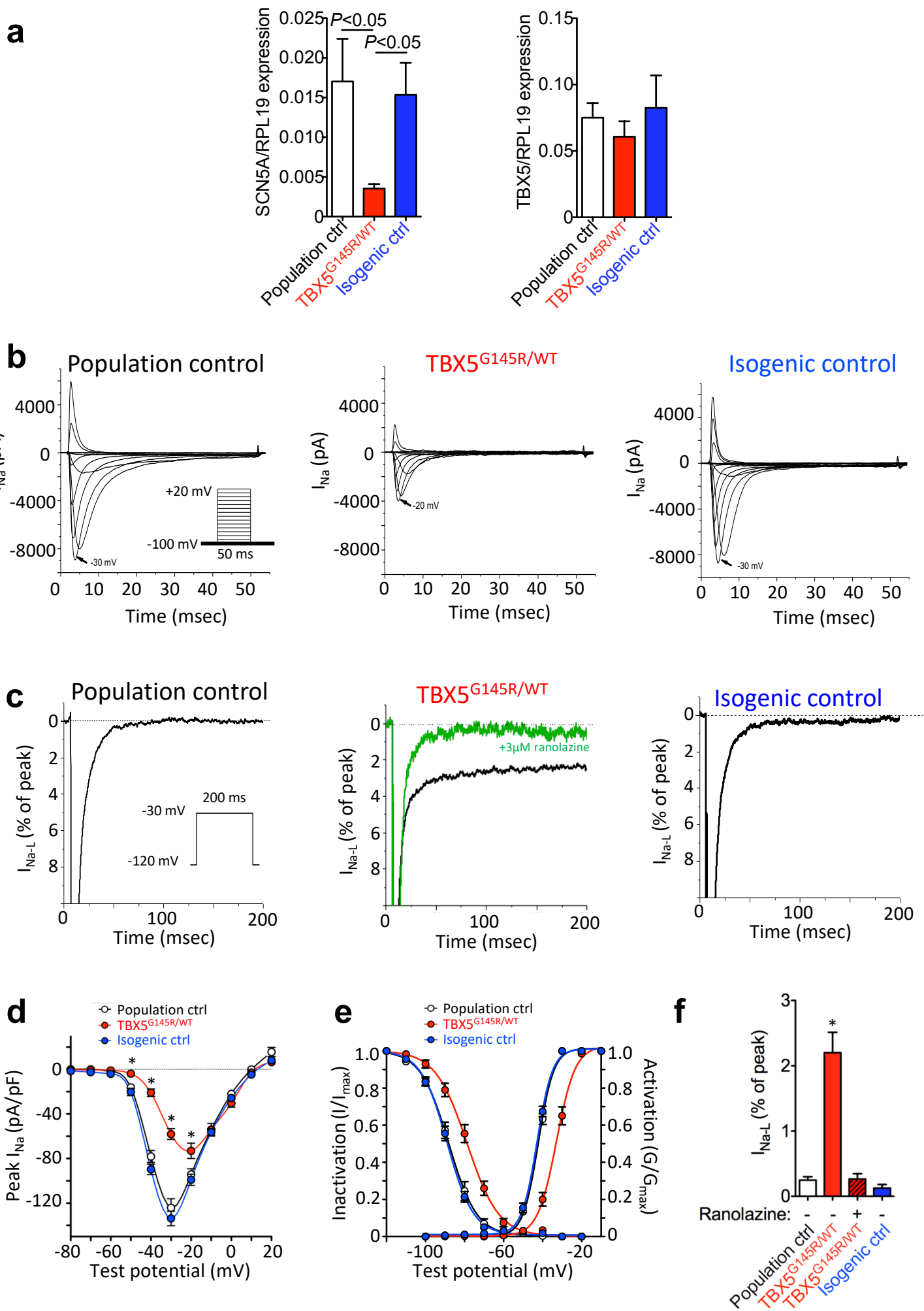
- pointes in the chronic atrioventricular block dog model. *Journal of the American College of Cardiology*. 2010;55:801-9.
67. Wu L, Ma J, Li H, Wang C, Grandi E, Zhang P, Luo A, Bers DM, Shryock JC and Belardinelli L. Late sodium current contributes to the reverse rate-dependent effect of IKr inhibition on ventricular repolarization. *Circulation*. 2011;123:1713-20.
68. Antzelevitch C, Belardinelli L, Zygmunt AC, Burashnikov A, Di Diego JM, Fish JM, Cordeiro JM and Thomas G. Electrophysiological effects of ranolazine, a novel antianginal agent with antiarrhythmic properties. *Circulation*. 2004;110:904-910.
69. Sakmann BF, Spindler AJ, Bryant SM, Linz KW and Noble D. Distribution of a persistent sodium current across the ventricular wall in guinea pigs. *Circ Res*. 2000;87:910-4.
70. El-Bizri N, Li CH, Liu GX, Rajamani S and Belardinelli L. Selective inhibition of physiological late Na(+) current stabilizes ventricular repolarization. *Am J Physiol Heart Circ Physiol*. 2018;314:H236-H245.
71. Ferrantini C, Pioner JM, Mazzoni L, Gentile F, Tosi B, Rossi A, Belardinelli L, Tesi C, Palandri C, Matucci R, Cerbai E, Olivotto I, Poggesi C, Mugelli A and Coppini R. Late sodium current inhibitors to treat exercise-induced obstruction in hypertrophic cardiomyopathy: an in vitro study in human myocardium. *Br J Pharmacol*. 2018;175:2635-2652.
72. Rajamani S, Liu G, El-Bizri N, Guo D, Li C, Chen XL, Kahlig KM, Mollova N, Elzein E, Zablocki J and Belardinelli L. The novel late Na(+) current inhibitor, GS-6615 (eleclazine) and its anti-arrhythmic effects in rabbit isolated heart preparations. *Br J Pharmacol*. 2016;173:3088-3098.
73. Karmakar CK, Khandoker AH, Voss A and Palaniswami M. Sensitivity of temporal heart rate variability in Poincare plot to changes in parasympathetic nervous system activity. *Biomedical engineering online*. 2011;10:17.
74. Dobin A, Davis CA, Schlesinger F, Drenkow J, Zaleski C, Jha S, Batut P, Chaisson M and Gingeras TR. STAR: ultrafast universal RNA-seq aligner. *Bioinformatics*. 2013;29:15-21.
75. Liao Y, Smyth GK and Shi W. featureCounts: an efficient general purpose program for assigning sequence reads to genomic features. *Bioinformatics*. 2014;30:923-30.
76. Zhao S, Guo Y, Sheng Q and Shyr Y. Advanced heat map and clustering analysis using heatmap3. *BioMed research international*. 2014;2014:986048.
77. Sheng Q, Zhao S, Guo M and Shyr Y. NGSPERL: a semi-automated framework for large scale next generation sequencing data analysis. *International Journal of Computational Biology and Drug Design*. 2015;8:203.
78. Mi H, Ebert D, Muruganujan A, Mills C, Albu L-P, Mushayamaha T and Thomas PD. PANTHER version 16: a revised family classification, tree-based classification tool, enhancer regions and extensive API. *Nucleic acids research*. 2020;49:D394-D403.
79. Kim D, Pertea G, Trapnell C, Pimentel H, Kelley R and Salzberg SL. TopHat2: accurate alignment of transcriptomes in the presence of insertions, deletions and gene fusions. *Genome biology*. 2013;14:R36.

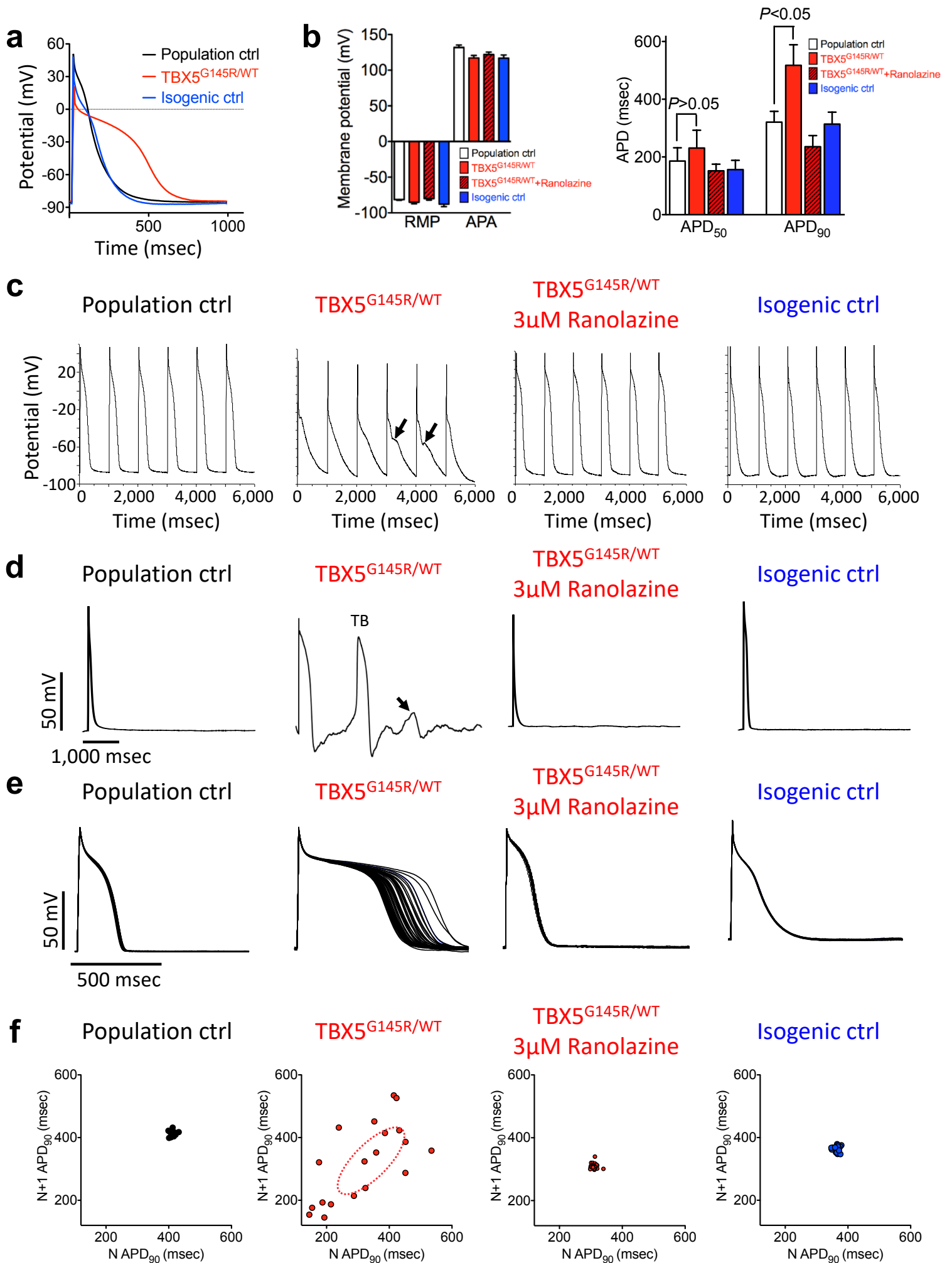
80. Barnett DW, Garrison EK, Quinlan AR, Stromberg MP and Marth GT. BamTools: a C++ API and toolkit for analyzing and managing BAM files. *Bioinformatics*. 2011;27:1691-2.
81. Kramer A, Green J, Pollard J, Jr. and Tugendreich S. Causal analysis approaches in Ingenuity Pathway Analysis. *Bioinformatics*. 2014;30:523-30.
82. Feinleib M, Kannel WB, Garrison RJ, McNamara PM and Castelli WP. The Framingham Offspring Study. Design and preliminary data. *Preventive medicine*. 1975;4:518-25.
83. Ngo D, Sinha S, Shen D, Kuhn EW, Keyes MJ, Shi X, Benson MD, O'Sullivan JF, Keshishian H, Farrell LA, Fifer MA, Vasan RS, Sabatine MS, Larson MG, Carr SA, Wang TJ and Gerszten RE. Aptamer-Based Proteomic Profiling Reveals Novel Candidate Biomarkers and Pathways in Cardiovascular Disease. *Circulation*. 2016;134:270-85.
84. Gold L, Ayers D, Bertino J, Bock C, Bock A, Brody EN, Carter J, Dalby AB, Eaton BE, Fitzwater T, Flather D, Forbes A, Foreman T, Fowler C, Gawande B, Goss M, Gunn M, Gupta S, Halladay D, Heil J, Heilig J, Hicke B, Husar G, Janjic N, Jarvis T, Jennings S, Katilius E, Keeney TR, Kim N, Koch TH, Kraemer S, Kroiss L, Le N, Levine D, Lindsey W, Lollo B, Mayfield W, Mehan M, Mehler R, Nelson SK, Nelson M, Nieuwlandt D, Nikrad M, Ochsner U, Ostroff RM, Otis M, Parker T, Pietrasiewicz S, Resnicow DI, Rohloff J, Sanders G, Sattin S, Schneider D, Singer B, Stanton M, Sterkel A, Stewart A, Stratford S, Vaught JD, Vrkljan M, Walker JJ, Watrobka M, Waugh S, Weiss A, Wilcox SK, Wolfson A, Wolk SK, Zhang C and Zichi D. Aptamer-based multiplexed proteomic technology for biomarker discovery. *PloS one*. 2010;5:e15004.
85. Puddu PE, Jouve R, Mariotti S, Giampaoli S, Lanti M, Reale A and Menotti A. Evaluation of 10 QT prediction formulas in 881 middle-aged men from the seven countries study: emphasis on the cubic root Fridericia's equation. *Journal of electrocardiology*. 1988;21:219-29.
86. Rautaharju PM, Mason JW and Akiyama T. New age- and sex-specific criteria for QT prolongation based on rate correction formulas that minimize bias at the upper normal limits. *International journal of cardiology*. 2014;174:535-40.
87. Badilini F and Sarapa N. Implications of methodological differences in digital electrocardiogram interval measurement. *Journal of electrocardiology*. 2006;39:S152-6.
88. Saque V, Vaglio M, Funck-Brentano C, Kilani M, Bourron O, Hartemann A, Badilini F and Salem JE. Fast, accurate and easy-to-teach QT interval assessment: The triplicate concatenation method. *Arch Cardiovasc Dis*. 2017;110:475-481.
89. London B, Michalec M, Mehdi H, Zhu X, Kerchner L, Sanyal S, Viswanathan PC, Pfahnl AE, Shang LL, Madhusudanan M, Baty CJ, Lagana S, Aleong R, Gutmann R, Ackerman MJ, McNamara DM, Weiss R and Dudley SC, Jr. Mutation in glycerol-3-phosphate dehydrogenase 1 like gene (GPD1-L) decreases cardiac Na⁺ current and causes inherited arrhythmias. *Circulation*. 2007;116:2260-8.
90. Antzelevitch C, Pollevick GD, Cordeiro JM, Casis O, Sanguinetti MC, Aizawa Y, Guerchicoff A, Pfeiffer R, Oliva A, Wollnik B, Gelber P, Bonaros EP, Jr., Burashnikov E, Wu Y, Sargent JD, Schickel S, Oberheiden R, Bhatia A, Hsu LF, Haissaguerre M, Schimpf R, Borggrefe M and Wolpert C. Loss-of-function mutations in the cardiac calcium channel underlie a new clinical entity characterized by ST-segment elevation, short QT intervals, and sudden cardiac death. *Circulation*. 2007;115:442-9.

91. Burashnikov E, Pfeiffer R, Barajas-Martinez H, Delpon E, Hu D, Desai M, Borggrefe M, Haissaguerre M, Kanter R, Pollevick GD, Guerchicoff A, Laino R, Marieb M, Nademane K, Nam GB, Robles R, Schimpf R, Stapleton DD, Viskin S, Winters S, Wolpert C, Zimmern S, Veltmann C and Antzelevitch C. Mutations in the cardiac L-type calcium channel associated with inherited J-wave syndromes and sudden cardiac death. *Heart rhythm : the official journal of the Heart Rhythm Society*. 2010;7:1872-82.
92. Crotti L, Marcou CA, Tester DJ, Castelletti S, Giudicessi JR, Torchio M, Medeiros-Domingo A, Simone S, Will ML, Dagradi F, Schwartz PJ and Ackerman MJ. Spectrum and prevalence of mutations involving BrS1- through BrS12-susceptibility genes in a cohort of unrelated patients referred for Brugada syndrome genetic testing: implications for genetic testing. *Journal of the American College of Cardiology*. 2012;60:1410-8.
93. Holst AG, Saber S, Houshmand M, Zaklyazminskaya EV, Wang Y, Jensen HK, Refsgaard L, Haunso S, Svendsen JH, Olesen MS and Tfelt-Hansen J. Sodium current and potassium transient outward current genes in Brugada syndrome: screening and bioinformatics. *The Canadian journal of cardiology*. 2012;28:196-200.
94. Watanabe H, Koopmann TT, Le Scouarnec S, Yang T, Ingram CR, Schott JJ, Demolombe S, Probst V, Anselme F, Escande D, Wiesfeld AC, Pfeufer A, Kaab S, Wichmann HE, Hasdemir C, Aizawa Y, Wilde AA, Roden DM and Bezzina CR. Sodium channel beta1 subunit mutations associated with Brugada syndrome and cardiac conduction disease in humans. *The Journal of clinical investigation*. 2008;118:2260-8.
95. Delpon E, Cordeiro JM, Nunez L, Thomsen PE, Guerchicoff A, Pollevick GD, Wu Y, Kanters JK, Larsen CT, Hofman-Bang J, Burashnikov E, Christiansen M and Antzelevitch C. Functional effects of KCNE3 mutation and its role in the development of Brugada syndrome. *Circulation Arrhythmia and electrophysiology*. 2008;1:209-18.
96. Hu D, Barajas-Martinez H, Medeiros-Domingo A, Crotti L, Veltmann C, Schimpf R, Urrutia J, Alday A, Casis O, Pfeiffer R, Burashnikov E, Caceres G, Tester DJ, Wolpert C, Borggrefe M, Schwartz P, Ackerman MJ and Antzelevitch C. A novel rare variant in SCN1Bb linked to Brugada syndrome and SIDS by combined modulation of Na(v)1.5 and K(v)4.3 channel currents. *Heart rhythm : the official journal of the Heart Rhythm Society*. 2012;9:760-9.
97. Verkerk AO, Wilders R, Schulze-Bahr E, Beekman L, Bhuiyan ZA, Bertrand J, Eckardt L, Lin D, Borggrefe M, Breithardt G, Mannens MM, Tan HL, Wilde AA and Bezzina CR. Role of sequence variations in the human ether-a-go-go-related gene (HERG, KCNH2) in the Brugada syndrome. *Cardiovascular research*. 2005;68:441-53.
98. Medeiros-Domingo A, Tan BH, Crotti L, Tester DJ, Eckhardt L, Cuoretti A, Kroboth SL, Song C, Zhou Q, Kopp D, Schwartz PJ, Makielski JC and Ackerman MJ. Gain-of-function mutation S422L in the KCNJ8-encoded cardiac K(ATP) channel Kir6.1 as a pathogenic substrate for J-wave syndromes. *Heart rhythm : the official journal of the Heart Rhythm Society*. 2010;7:1466-71.
99. Kattygnarath D, Maugenre S, Neyroud N, Balse E, Ichai C, Denjoy I, Dilanian G, Martins RP, Fressart V, Berthet M, Schott JJ, Leenhardt A, Probst V, Le Marec H, Hainque B, Coulombe A, Hatem SN and Guicheney P. MOG1: a new susceptibility gene for Brugada syndrome. *Circulation Cardiovascular genetics*. 2011;4:261-8.
100. Ohno S, Zankov DP, Ding WG, Itoh H, Makiyama T, Doi T, Shizuta S, Hattori T, Miyamoto A, Naiki N, Hancox JC, Matsuura H and Horie M. KCNE5 (KCNE1L)

- variants are novel modulators of Brugada syndrome and idiopathic ventricular fibrillation. *Circulation Arrhythmia and electrophysiology*. 2011;4:352-61.
101. Giudicessi JR, Ye D, Tester DJ, Crotti L, Mugione A, Nesterenko VV, Albertson RM, Antzelevitch C, Schwartz PJ and Ackerman MJ. Transient outward current (I_{to}) gain-of-function mutations in the KCND3-encoded Kv4.3 potassium channel and Brugada syndrome. *Heart rhythm : the official journal of the Heart Rhythm Society*. 2011;8:1024-32.
102. Ishikawa T, Sato A, Marcou CA, Tester DJ, Ackerman MJ, Crotti L, Schwartz PJ, On YK, Park JE, Nakamura K, Hiraoka M, Nakazawa K, Sakurada H, Arimura T, Makita N and Kimura A. A novel disease gene for Brugada syndrome: sarcolemmal membrane-associated protein gene mutations impair intracellular trafficking of hNav1.5. *Circulation Arrhythmia and electrophysiology*. 2012;5:1098-107.
103. Liu H, Chatel S, Simard C, Syam N, Salle L, Probst V, Morel J, Millat G, Lopez M, Abriel H, Schott JJ, Guinamard R and Bouvagnet P. Molecular genetics and functional anomalies in a series of 248 Brugada cases with 11 mutations in the TRPM4 channel. *PLoS One*. 2013;8:e54131.
104. Riuro H, Beltran-Alvarez P, Tarradas A, Selga E, Campuzano O, Verges M, Pagans S, Iglesias A, Brugada J, Brugada P, Vazquez FM, Perez GJ, Scornik FS and Brugada R. A missense mutation in the sodium channel beta2 subunit reveals SCN2B as a new candidate gene for Brugada syndrome. *Human mutation*. 2013;34:961-6.
105. Fukuyama M, Ohno S, Makiyama T and Horie M. Novel SCN10A variants associated with Brugada syndrome. *Europace : European pacing, arrhythmias, and cardiac electrophysiology : journal of the working groups on cardiac pacing, arrhythmias, and cardiac cellular electrophysiology of the European Society of Cardiology*. 2016;18:905-11.
106. Hu D, Barajas-Martinez H, Pfeiffer R, Dezi F, Pfeiffer J, Buch T, Betzenhauser MJ, Belardinelli L, Kahlig KM, Rajamani S, DeAntonio HJ, Myerburg RJ, Ito H, Deshmukh P, Marieb M, Nam GB, Bhatia A, Hasdemir C, Haissaguerre M, Veltmann C, Schimpf R, Borggrefe M, Viskin S and Antzelevitch C. Mutations in SCN10A are responsible for a large fraction of cases of Brugada syndrome. *Journal of the American College of Cardiology*. 2014;64:66-79.







a

Wild-type *SCN5A* allele (p.H508H):

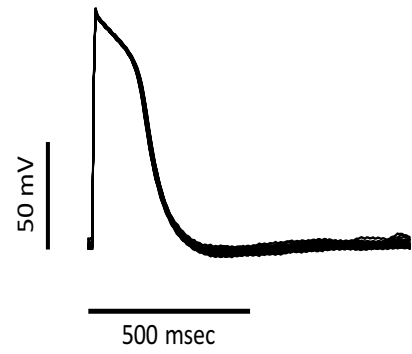
DNA seq: 5' - GAAGATGGTCCCAGAGCAATGAATCATC - 3'

Amino acid: E D G P R A M N H

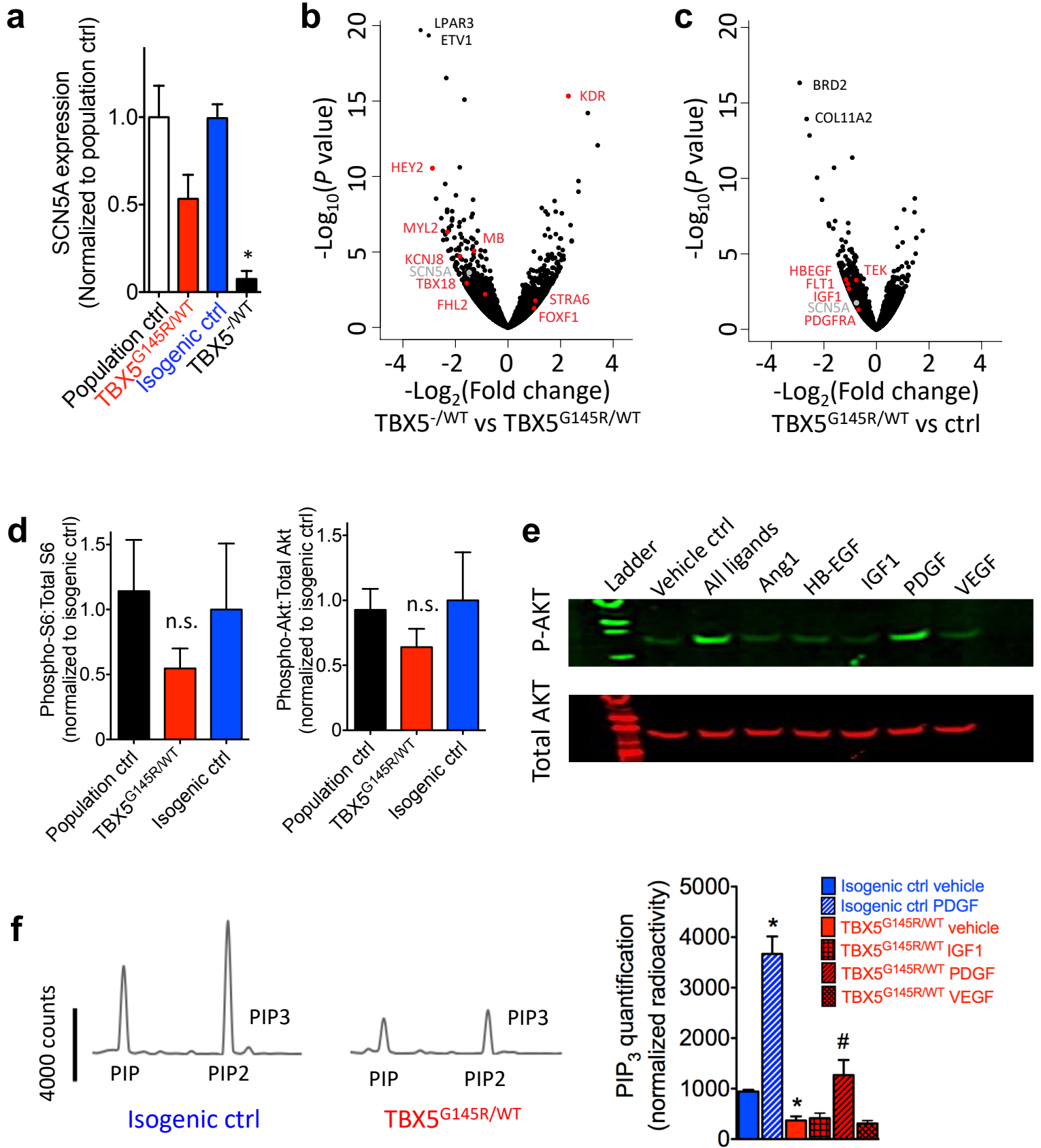
Mutant *SCN5A* allele (frameshifting indel):

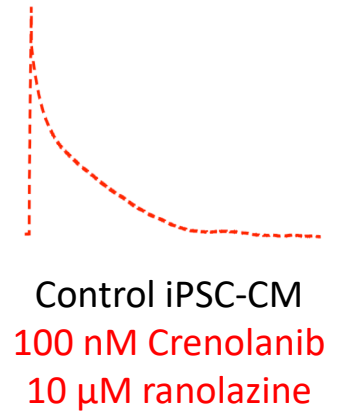
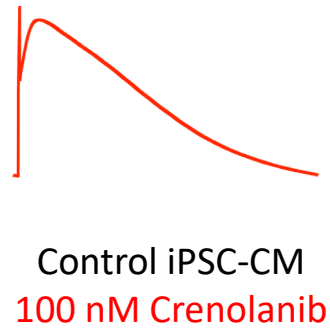
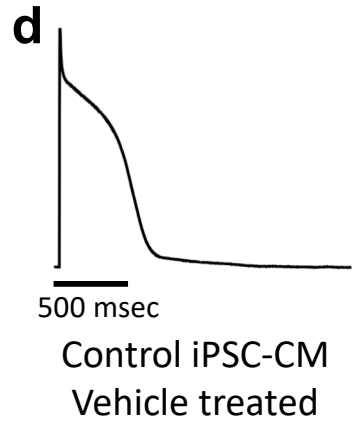
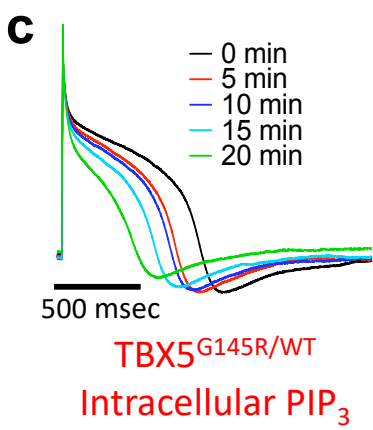
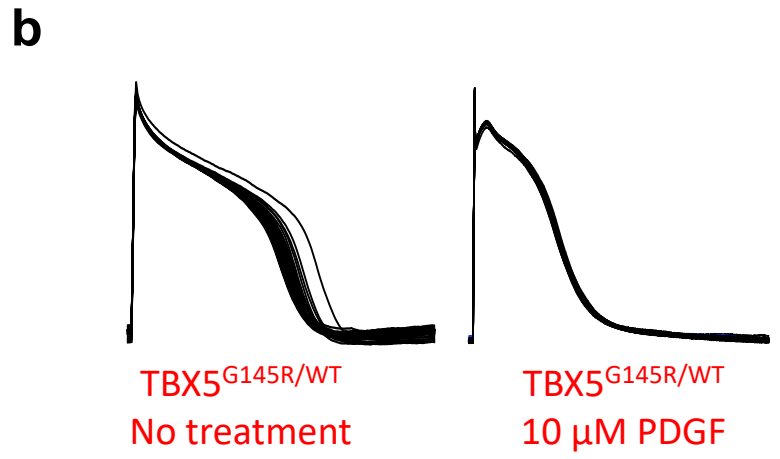
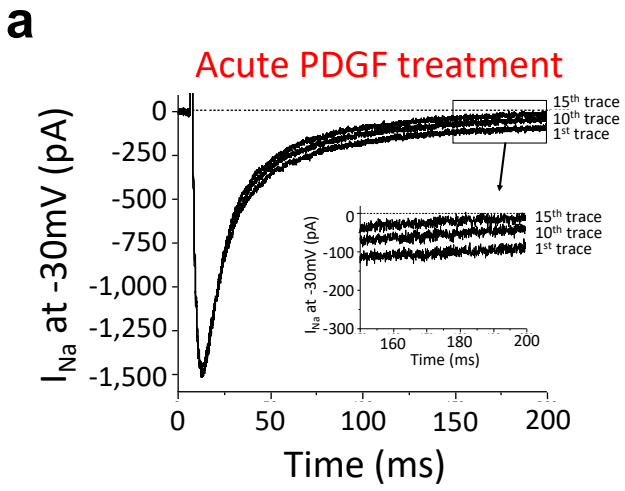
DNA seq: 5' - GAAGATGGTCCCAGAGCAATGAAATAA - 3'

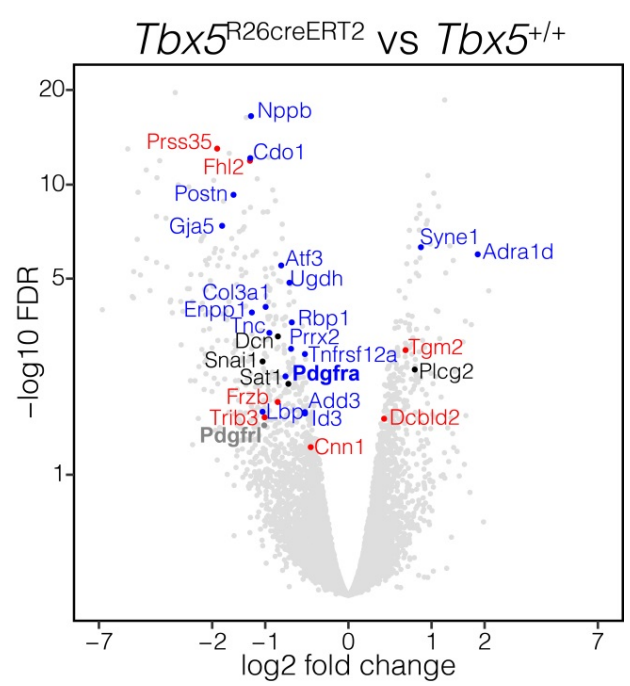
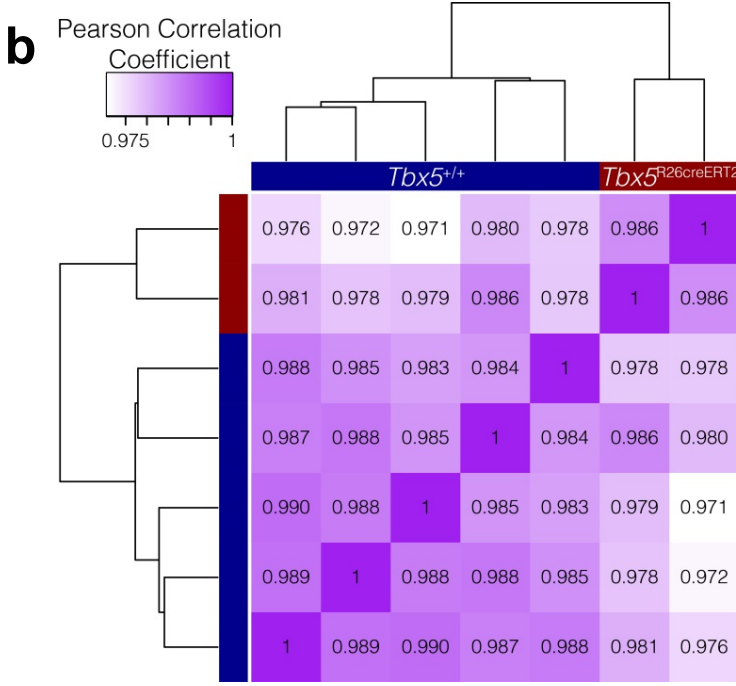
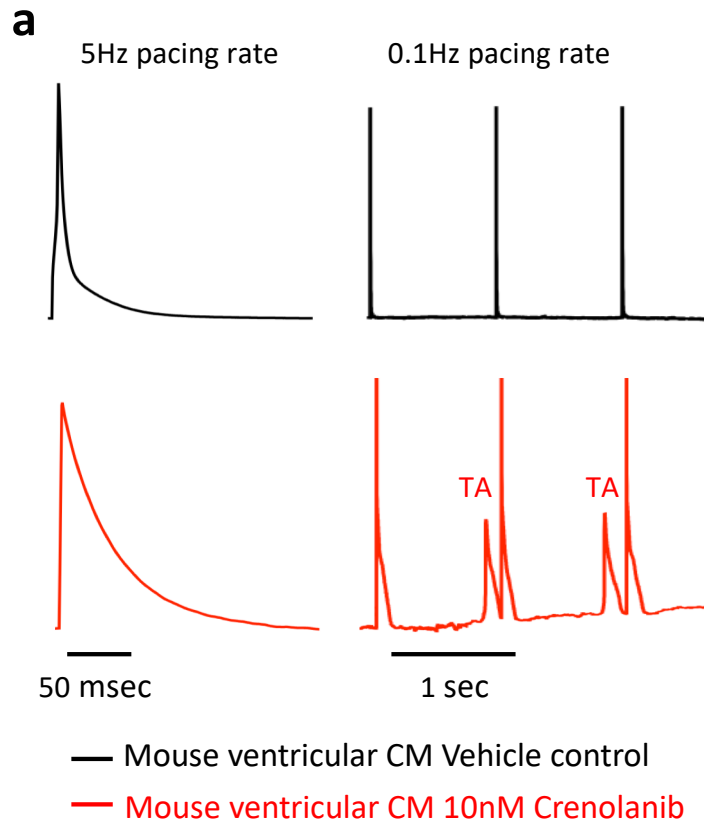
Amino acid: E D G P R A M K X

b

Human iPSC-CMs
SCN5A^{-/WT}; *TBX5*^{WT/WT}







a

